2015

A Heterogeneous Aerial Platform Mission Planner using a Genetic Algorithm

Jonathan Rojas

A Heterogeneous Aerial Platform Mission Planner using a Genetic Algorithm

Jonathan Rojas

Thesis submitted to the Statler College of Engineering and Mineral Resources at West Virginia University in partial fulfillment of the requirements for the degree of

Masters of Science in Mechanical Engineering

Jay Wilhelm, Ph.D., Chair
Marvin Cheng, Ph.D.
Marjorie Darrah, Ph.D.
Mario Perhinschi, Ph.D.

Department of Mechanical and Aerospace Engineering

Morgantown, West Virginia
2015

Keywords: Unmanned Aerial Vehicle, UAV, Path Planning, Genetic Algorithm

Abstract

A Heterogeneous Aerial Platform Mission Planner using a Genetic Algorithm

by Jonathan Rojas

Systems exist today that can plan a mission with more than one aircraft efficiently for surveillance. However, objectives in these missions do not change and are typically performed using a homogeneous set of aerial vehicles. An adaptive mission planner was sought to task a heterogeneous set of Unmanned Aerial Vehicles (UAVs) when an unknown Target of Interest (TOI) is located amongst a set of Points of Interest (POIs). First, two dimensional flight path models of fixed wing and quadcopter platforms were created. Next, the design of a genetic algorithm and its fitness functions were studied. Fixed wing fitness functions were developed to balance POI task loads amongst a set of fixed wing aircraft. A quadcopter fitness function was then designed to task a quadcopter to visit a newly located TOI. The quadcopter fitness function was also designed to maximize battery usage as it was desired that the quadcopter visit as many additional POIs on route to and from the TOI. Case studies were then simulated using varying heterogeneous UAV sets and TOI locations. Results of these simulations were then analyzed using mission times as a performance metric. Simulation results indicated that the deployment of the quadcopter to the TOI and additional POIs reduced overall mission times. Mission time reductions were also found to be depended on the number of fixed wing aircraft used in heterogeneous UAV sets.

Acknowledgements

This research project would not have been possible without the help and support of many people. I would like to foremost thank my advisor Dr. Jay Wilhelm. Without his patience, guidance and knowledge during my Masters Degree none of this would have been possible.

I would also like to thank my committee members Dr. Marvin Cheng, Dr. Marjorie Darrah and Dr. Mario Perhinschi for their suggestions and edits on this thesis.

I would lastly like to thank my family for all the love and support they have given me during my time here at WVU. I would not be where I am today without their love and support.

Sincerely,

Jonathan Rojas

Contents

List of Figures

List of Tables

Abbreviations

UAV	**U**nmanned **A**erial **V**ehicle
POI	**P**oint **O**f **I**nterest
TOI	**T**arget **O**f **I**nterest
VTOL	**V**ertical **T**ake-**O**ff and **L**anding
GA	**G**enetic **A**lgorithm

Chapter 1

Introduction

Unmanned Aerial Vehicles (UAVs) have become an important resource for Intelligence, Surveillance and Reconnaissance (ISR) missions in military operations. Ground teams have access to multiple UAVs but typically only use one UAV at a time. However, multiple UAVs in an ISR mission could increase coverage area and reduce mission times. Systems exist that can plan a mission with more than one UAV to search a set of Points of Interest (POIs). However, these systems do not typically account for a scenario in which an unknown Target of Interest (TOI) is located during a mission and only utilize a homogeneous set of UAVs. A human operator may have to manually re-task the UAVs in the event that a TOI is found. The TOI may represent a POI or a separate spot along the UAV flight path which requires long term or closer surveillance. **Due to this need, an adaptive mission planner was sought to task a heterogeneous set of UAVs when an unknown TOI is located amongst a set of POIs.**

Adaptive mission plans will be produced using either fixed wing aircraft or a combination

of both fixed wing aircraft and quadcopter platforms. Initially, fixed wing aircraft will be used to perform overhead fly-by visitations of multiple POIs as they are capable of achieving long duration flight times. POI task loads will be balanced amongst the fixed wing aircraft set to maximize POI coverage area. Once a TOI is located by the fixed wing aircraft set, a quadcopter will be deployed to visit the TOI as they can Vertically Take Off and Land (VTOL) making them ideal for long term ground surveillance. Upon arriving at the TOI, the quadcopter will deploy a sensor pod to provide long term ground surveillance. Additional unsearched POIs will also be visited by the quadcopter by tasking it to visit nearby POIs on route to and from the TOI. Remaining unsearched POIs will then be re-distributed amongst the fixed wing aircraft set. Allowing the quadcopter to visit unsearched POIs after the TOI has been found could reduce the number of POIs visited by the fixed wing platforms and the overall mission time duration.

In order to develop the adaptive mission planner, literature will first be collected on tasking and path planning algorithms. Tasking algorithms will be investigated to determine a method of generating initial and mission re-plan solutions. Path planning algorithms will be studied to select a method of constructing fixed wing and quadcopter flight paths. Next, an adaptive mission planner will be designed using the selected tasking and path planning methods. Case studies will then be simulated by varying the number of fixed wing aircraft in the heterogeneous set and the location of a single unknown TOI. Simulating case studies will ensure that the adaptive mission planner generates mission that satisfy both initial and mission re-plan objectives. Results of the simulations will then be analyzed using mission times as a performance metric.

Chapter 2

Review of Literature

In order to develop the adaptive mission planner, background research was necessary in the following areas: UAV platforms, tasking algorithms and path planning algorithms. First, UAV platforms were studied to determine which UAV platforms were best suited to search POIs and TOIs. Next, tasking algorithms were studied to determine a method which could be used to generate initial and mission re-plan solutions. Lastly, path planning algorithms were examined to determine a method of generating two dimensional fixed wing and multirotor helicopter flight paths.

2.1 Unmanned Aerial Vehicles

An Unmanned Aerial Vehicle is defined as an aircraft that does not carry a pilot or crew on board and can fly autonomously using a pre-programmed flight plan and aircraft

dynamic control systems [3]. UAVs can be found in a variety of airframe configurations including fixed wing and multirotor helicopter configurations [4]. Each configuration has advantages and disadvantages in performance and maneuverability when compared to each other.

2.1.1 Fixed Wing Aircraft

Fixed wing aircraft use a set of stationary wings to generate lift and achieve flight [5]. Control surfaces on these wings control the orientation of the aircraft. Aileron surfaces control the roll, elevator surfaces control the pitch and rudder surfaces control the yaw orientation of the aircraft. Forward motion of the aircraft is achieved by either gliding over moving air or by thrust produced via a propeller or engine. Fixed wing aircraft can achieve long duration flight times and high efficiency due to their body lifting surfaces which makes them idea for long duration ISR missions. Disadvantages of fixed wing aircraft includes the requirement of a flat surface to take-off and land. Additionally, air must be moving over their wings to generate lift and thus requires them to always remain in a constant forward motion. An example of a fixed wing UAV is the AeroVironment RQ-11 Raven [6] which has a flight time of 60-90 minutes and a wingspan of 1.4 meters as seen in Figure 2.1. Fixed wing aircraft can be utilized in this application to search multiple POIs as they are capable of long duration flight times.

FIGURE 2.1: AeroVironment RQ-11 Raven UAV

2.1.2 Multirotor Helicopters

Multirotor helicopters feature multiple rotors which induce thrust used for lifting [5]. Rotors are fixed in a circular configuration around a central body. Roll, pitch and yaw control of a multirotor helicopter is achieved by varying the thrust produced by each rotor. A primary advantage of multirotor helicopter is a VTOL ability which typically allows them to hover and achieve low speed flight [7]. Disadvantage of a multirotor helicopter includes the increase in power consumption due to the varying propeller thrust used to lift the vehicle. Increased power consumption may result in shorter overall flight times. An example of a four-rotor multirotor helicopter is the Aeryon Scout Quadcopter [8] seen in Figure 2.2. Multirotor helicopters can be used in this application as they have the capability of hovering and deploying a sensor pod to provide additional surveillance of the TOI.

FIGURE 2.2: Aeryon Scout Quadcopter

2.1.3 Unmanned Aerial Vehicle Comparisons

Fixed wing aircraft are best suited for applications where long duration flight times greater than 60 minutes are desired such as in a long duration ISR mission. Multirotor helicopters are best suited when a VTOL vehicle is desired such as in a loitering or close surveillance application. Tasking methods will be investigated next to determine which method will be best to generate mission plan solutions.

2.2 Tasking Algorithms

Literature was collected on tasking algorithms to examine which methods could be used to generate initial and mission re-plan solutions. Tasking methods found in literature included: Mixed Integer Linear Programming (MILP), Dijkstra's Algorithm (DA) and Genetic Algorithms (GAs). MILP will be presented first followed by DA.

2.2.1 Mixed Integer Linear Programming

MILP aims to either maximize or minimize variables of a linear objective function [9]. Linear inequalities and equality constraints along with bounds are placed on the objective function variables. In comparison to traditional linear programming methods in which variables can be all real numbers, some or all MILP variables must be integers. To illustrate a basic example, an objective function in which variables x_1 and x_2 must be minimized can be seen in Equation 2.1.

$$\min_x(-1x_1 - 1x_2) \tag{2.1}$$

Constraints are then placed on the variables where both x_1 and x_2 must be integers using Equations 2.2 and 2.3.

$$x_1 + 4x_2 \leq 20 \tag{2.2}$$

$$6x_1 + 2x_2 \leq 25 \tag{2.3}$$

Lastly, bounds are placed on the variables using Equations 2.4 and 2.5.

$$0 \leq x_1 \tag{2.4}$$

$$0 \leq x_2 \tag{2.5}$$

MILP can be used to design tasking objective functions which can be subjected to mission constraints and bounds. Richards, Bellingham, Tillerson and How [10] applied MILP

to model optimization task assignments for UAVs under vehicle capability constraints. Schumacher, Chandler and Pachter [11] applied MILP to a scenario in which multiple UAVs were required to classify geographically dispersed targets under timing and task order constraints. Darrah, Niland and Stolark [12] extended the work in [11] by adding new constraints that increased the complexity of the task allocation problem to include dynamic re-tasking. Added assumptions and constraints included survivable vehicle models after unmanned combat and dynamic target discovery. Wang, Zhang, Geng, Fuh and Teo [13] also applied MILP to task a heterogeneous set of fixed winged like UAVs to accomplish a set of heterogeneous tasks.

MILP could be applied to solve the initial mission planning problem for this application under the constraint of balanced POI tasking amongst a homogeneous set of UAVs. On the other hand, MILP has also been shown to be undesirable due to its long computational times required to solve larger scale problems [14]. Such a characteristic could hinder computational times as the number of POIs in a mission increases. Next, Dijkstra's Algorithm (DA) will be presented to illustrate how it has been implemented to solve tasking problems.

2.2.2 Dijkstra's Algorithm

Dijkstra's Algorithm (DA) was developed by computer scientist Edsger Wybe Dijkstra in 1956 [15] with the goal of finding the shortest path between a starting node (R1) and goal node (R2) using a weighted graph approach. Initially, a set of neighboring nodes

around the starting node is considered [16]. All the neighboring nodes in the graph are placed in a priority queue which is prioritized by distance, or weight, between the current node (T-node) and its neighboring nodes. The path to the neighboring node with the shortest distance is selected and the neighboring node is assigned as the current (T-node). Distances to a new set of neighboring nodes are then calculated and the queue is updated. This procedure is repeated until the shortest path from the starting node (R1) to the goal node (R2) is found. A flowchart illustrating DA can be seen in Figure 2.3 [17]. Applications of DA can be found in software protocols [18], power restoration systems [19] and emergency vehicle routing [20].

DA appears to be best suited for applications where the shortest path between a series of nodes is desired and thus it may not be a good fit for generating initial and mission re-plans. DA may not work for this application as mission plans will not seek the shortest paths but rather paths that fulfill a set of mission objectives.

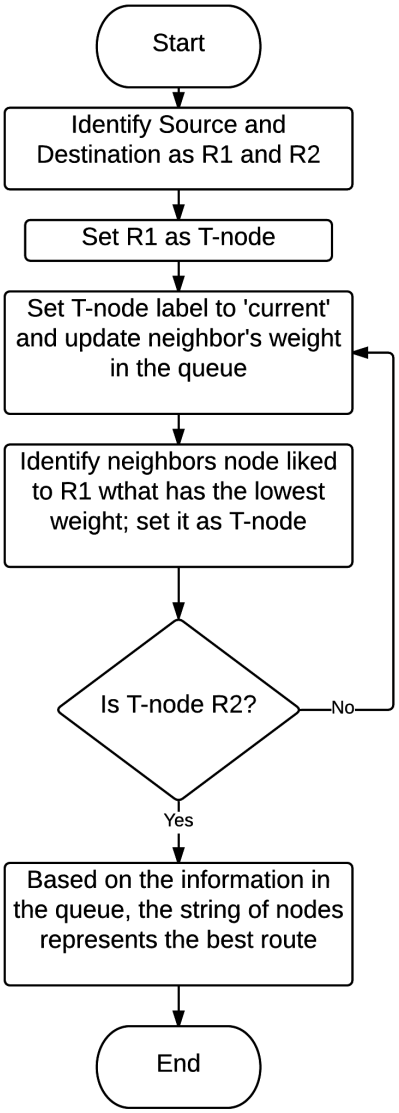

FIGURE 2.3: Dijkstra's Algorithm Flowchart

2.2.3 Genetic Algorithms

Genetic Algorithms (GA) are based of Charles Darwin's evolutionary theory of "survival of the fittest" [21]. Darwin's theory proposes that a species exists in nature today as a result of years of adaptation in a forever changing environment. Individuals that learned

to adapt to their environment had a better chance of survival and as a result, were able to procreate offspring that carried these adaptive traits. Over time, an entire population of that species can be said to have "evolved" to contain the better fit species.

GAs search for an optimized solution that either maximizes or minimizes parameters used to characterize a solution in the structure of a chromosome. Typically, a GA will begin by initializing a randomly generated population of potential chromosome/solutions [22]. Solutions are then evaluated by means of a fitness function and are assigned a quantitative score.

Convergence of the GA can then be checked via means of a convergence criterion. In some cases, an imposed number of GA generations must be satisfied or a desired fitness score within the population must be satisfied.

If GA convergence has shown to be unsatisfied, the best fit individuals of the current population are selected and reproduce as "parents" into a new population. Roulette-wheel selection methods are probabilistic methods of determining which individuals will contribute to the next population based on fitness score[23]. Elitism can also be implemented, which passes an unaltered copy of the best fit solution of each population into the succeeding population. Passing an unaltered copy may ensure that solutions do not degrade in fitness from one generation to the next.

Genetic operations are then performed on the selected population to produce a new population of solutions. Crossover operators split two "parent" chromosomes at randomized locations to create two "children" chromosomes. A single chromosome is generated by

concatenating the first part of one chromosome and the second part of the other chromosome. Mutation operators alter a number of elements in the chromosomes based on a mutation rate. Once these alterations have been performed, the current population now contains a set of "children" chromosomes which represent the new population. GA generations are repeated until a convergence criterion is met or until a superimposed number of generations has been achieved. Figure 2.4 illustrates a flowchart of the GA.

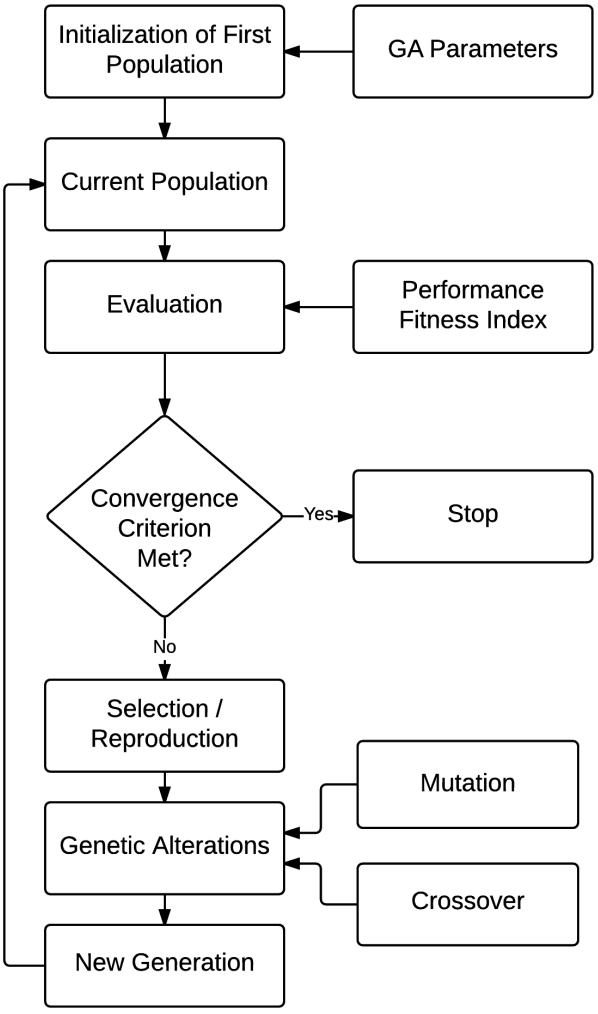

FIGURE 2.4: Genetic Algorithm Framework

2.2.3.1 GA's for UAV Tasking

Jing Tian [24] took a GA approach to a multi-UAV cooperative reconnaissance mission planning problem. The objective of this work was to conduct UAV reconnaissance on a set of targets within a specified window of time. Fitness evaluations penalized solutions that failed to visit the targets within the specified window of time and those that exceeded the maximum allowed UAV travel time. In contrast, Darrah [25] applied the GA to generate mission plans that tasked a homogeneous set of UAVs in a long term balanced surveillance mission. In this work, a set of AeroVironment Raven UAVs, seen in Figure 2.5, were cooperatively tasked to survey a set of POIs in a search space. A fixed wing aircraft fitness function was designed to maximize mission surveillance times while balancing POI visitation loads amongst the UAVs In the set.

FIGURE 2.5: AeroVironment Raven UAV

An expanded study of Darrah's GA application examined the performance of the GA, in parallel executions, in converging to a "good" solution by varying the number of generations and population sizes [26]. A "good" solution was defined as a fitness score that

came within a confidence range of the highest fitness score attained over all GA runs. Parallel operations of the same GA with identical parameters over 50,000 generations obtained the highest fitness score. Confidence range was defined as the number of generations needed to ensure that all generations will achieve at least 90% of the highest fitness score. Results of this study indicated, that as the population size increased, fewer generations were needed to reach a 90% confidence range. Results found that GA run times increased due to the larger population sizes and can be seen in Table 2.1. GAs have been shown to be used extensively in UAV tasking and this would be a suitable option for this application.

Population Size	Generation Run Time (min.)	Minutes/ Generation	Generations to 90% Confidence	Time (min.) to 90% Confidence
25	23.255	0.0047	133	0.619
35	28.348	0.0057	106	0.601
45	35.310	0.0071	91	0.646
50	41.391	0.0083	82	0.679
60	50.251	0.0101	74	0.744
70	58.140	0.0116	91	1.058
80	68.378	0.0137	84	1.149
90	74.647	0.0149	78	1.162
100	84.327	0.0169	75	1.267
200	150.650	0.0301	46	1.386

TABLE 2.1: Population Size and Generations to 90% Confidence

Based on the number of GA applications in UAV tasking, GAs display great promise to generate initial and mission re-plan solutions for the proposed application. Existing GA applications for a balanced surveillance missions could be used as a basis for initial mission planning. Development of a re-plan fitness function can then be used to evaluate potential re-plan solutions.

2.2.4 Tasking Algorithm Comparisons

MILP has been shown to generate optimized solutions under a series of constraints, yet MILP is limited due to high computational times. DA is best in finding the shortest path between a series of nodes. GAs can also obtain optimized mission plan solutions and evaluate solutions via a customizable functions. Path planning methods will be investigated next to determine what method would be best to generate fixed wing and quadcopter flight paths.

2.3 Path Planning Algorithms

Path planning is the process of formulating a route that moves an entity from an initial state to a final state in two or three dimensional environment, based of vehicle dynamics and navigational requirements [27]. Road map methods will be presented first followed by pose-based methods.

2.3.1 Road Map Methods

Road map path planning methods break down a solution space into a finite number of discrete segments. A desired mission optimization criterion is then used to select an optimal path in the solution space. Common road map methods include the Voronoi diagram and cell decomposition.

2.3.1.1 Voronoi Diagram

Voronoi diagram methods use a set of points in a two dimensional space as an input and generates lines, or paths, that are equidistant between two nearby points [28]. Path segments that converge around each point form a set of polygons and the shortest vertices belonging to each polygon represent the shortest path.

Bhattacharya and Gavrilova [29] used the Voronoi diagram representation to find the shortest path between a source and a destination in the presence of simple polygon obstacles. Pei-bei, Zuo-e and Jun [30] applied the Voronoi diagram method to describe threat environments and no-fly zones for UAV dynamic path planning. Path segments that fell in a no-fly zone were removed from the map. Flyable UAV paths were then generated by filleting the resulting path segments at their intersections using a radius equal to the UAVs minimum turn radius. In contrast, Davis [31] implemented the Voronoi diagram to generate collision free paths through a series of cylindrical risk zones. However, this method was formulated such that there was no need to remove path segments in risk zones which reduces the likelihood of obtaining no available path. Voronoi diagrams may not be suitable for this application as there is no need to generate the shortest path or a path avoiding obstacles in the search space.

2.3.1.2 Cell Decomposition

Cell decomposition consists of breaking down a solution space into a uniform grid of nodes and segments that form cells. Nodes and segments that fall inside threat or obstacle

zones can be removed from the solutions space. Two dimensional applications of the cell decomposition are common however it can be expanded to three dimensions as well.

Araujo, Sujit and Sousa applied the cell decomposition method to generate a flight path for a UAV tasked to collect aerial coverage [32]. In this work, a method was developed to determine the optimal number of path lanes needed within the cells to minimize UAV turns while providing complete coverage of the search space. Perhinschi [33] applied the cell decomposition method to produce a grid search space containing obstacles. Cells and path segments that fell within these obstacle zones were removed from the grid. Dijkstra's algorithm was then applied to determine the optimal path through the available nodes. Resulting paths produced a flyable trajectory by filleting intersecting paths similar to Pei-bei, Zuo-e and Jun [30]. Similar to Voronoi Diagrams, cell decomposition may not be suitable for this application as there is no need generate a path which avoids obstacles in the search space.

2.3.2 Pose-Based Methods

Pose-based path planning methods consist of generating a path that traverses a series of specified waypoints in space. These methods are not dependent based upon the shortest overall path distance, but rather the order in which these waypoints must be traversed. The minimum distance is then found between the consecutive waypoints in the series. Two notable pose-based path planning methods is the Dubins and the Clothoid method.

2.3.2.1 Dubins

Dubins pose-based path planning algorithm was developed by L.E. Dubins in 1957 [34]. Dubins methods use a combination of circular arcs, of a constant radius, and straight line segments to generate a path. Arcs and straight path segments are then connected to each other via relevant tangent points to construct a full path.

Grymin and Crassidis [35] have applied the Dubins method to construct a flyable trajectory for a UAV tasked to navigate through a series of waypoints. In the study, a simplified aircraft model was constructed under the assumptions of constant velocity and turn radius.

Karas [36] implemented the Dubins paradigm to model a two dimensional fixed wing aircraft flight path. In this work, a fixed wing aircraft flight path was modeled through a series of POIs in a search space. Dubins arcs express bank maneuvers and Dubins straight path segments expressed forward paths. Bank maneuvers were modeled as paths equal to the aircraft minimum turn radius at the aircraft cruising speed. One second sampling rates were used to calculate the flight path segments. Sampling the flight path at this rate ensured that computational efforts of the algorithm were kept to a minimum while maintaining the curvature needed to describe the flyable path.

Generating the flight path was achieved via an algorithm that generated a new trajectory point and path segment at each time step. Figure 2.6 illustrates a logical flowchart of this algorithm. Each trajectory point calculated corresponded to the start and the end of a path segment. Figure 2.7 illustrates the segments that are expressed by a forward

path velocity vector $\overrightarrow{v}$ in the direction of the aircraft current heading angle α. Bearing angle, β, represented the angle between a consecutive POI relative to a current POI or location.

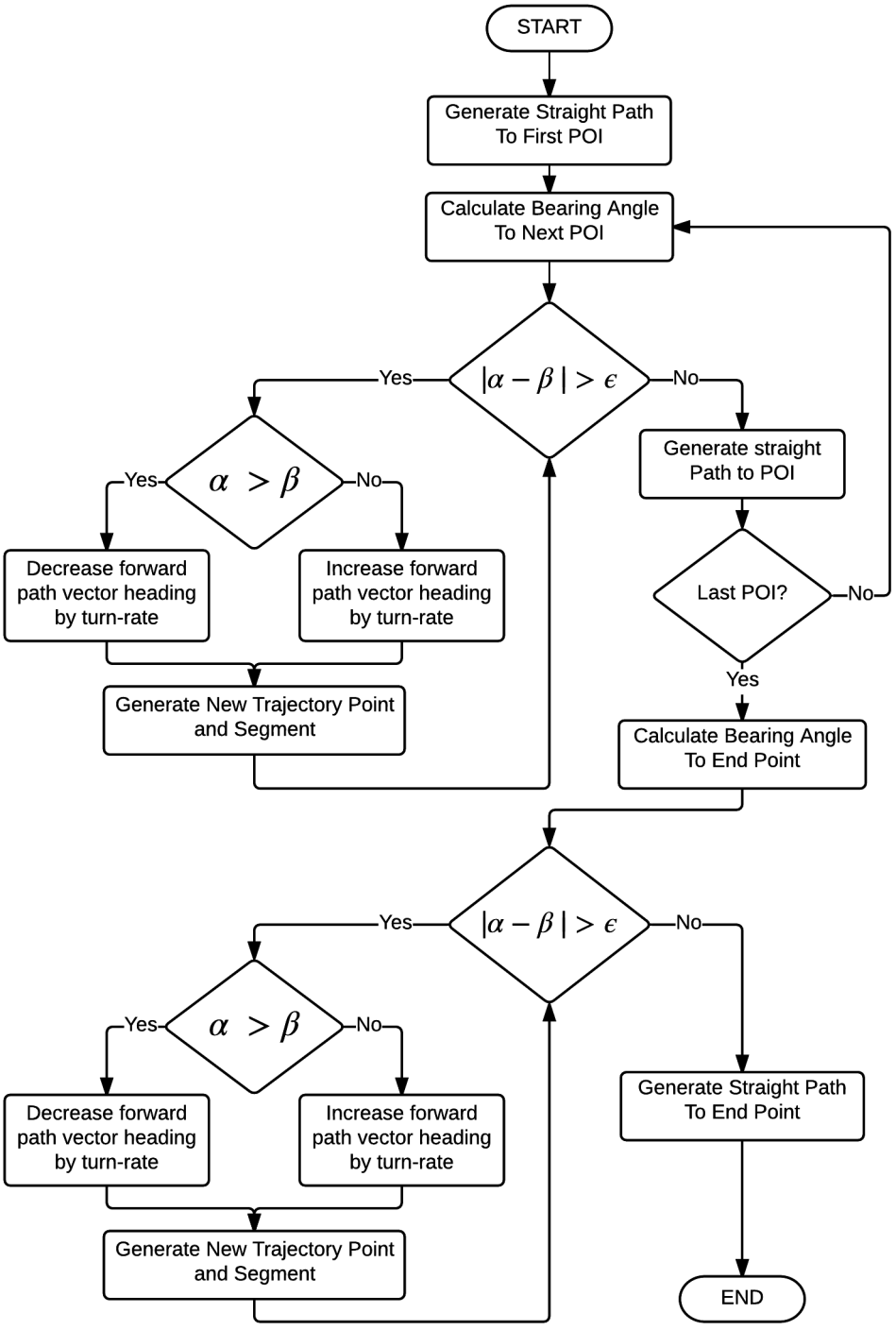

FIGURE 2.6: Fixed Wing Path Planner Flowchart

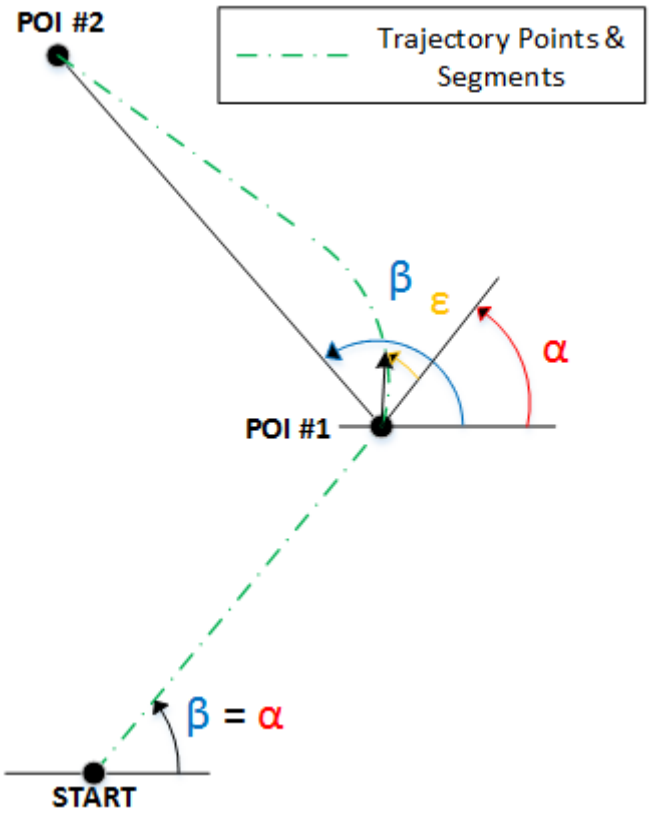

FIGURE 2.7: Path Segmentation and Angle

To begin, a bearing angle β to the first POI relative to the aircraft current position was calculated. Aircraft heading angle α was then set equal to the bearing angle β as the aircraft was initially assumed to be inbound towards the first POI. Straight path segments were generated until the first POI was reached. Once the aircraft reached the first POI, the algorithm determined the difference between the aircraft current heading angle α and the bearing angle β to the next POI. The difference between angle α and β was compared to the aircraft turn-rate angle ϵ which was the maximum angle that aircraft could turn at each time step. If the difference between the angles was found to be larger than the turn-rate angle ϵ, the aircraft heading angle α was adjusted by adding or subtracting

the turn-rate angle ϵ. Aircraft heading was incrementally adjusted until the difference between the heading angle α and bearing angle β was smaller than the turn-rate angle ϵ. At this point, the aircraft was in a straight line path with the next POI and straight path segments were generated.

Davis [33] applied the Dubins paradigm to create a UAV path through a series of points not based on shortest total distance, but rather the order of visitation and distance between consecutive points. Visitation of points were defined as being either "observing" or "visiting". Observing a point consisted of generating a circular path that flew around an event zone. Visiting a point consisted of generating a path that flew through the point. The Dubins paradigm would be best suited for this application as the generated path can not only traverse a specific series of waypoints, but can be used to model two-dimensional flight paths for both fixed wing and quadcopter platforms.

2.3.2.2 Clothoid

Clothoid paths are similar to the Dubins method however, arc paths are represented using a continuous curvature profile. In some cases, Clothoid methods are preferred to model UAV flight paths when compared to the Dubins method. Using a Clothoid continuous curvature profile results in a gradual or ramp acceleration profile that may be easier for commonly used UAV platforms to follow.

Wilburn [37] developed a three dimensional UAV Clothoid trajectory generation algorithm which produced flyable paths of continuous curvature that ensured a more followable command path. This method was developed as an extension of the three dimensional Dubins and two dimensional Clothoid methods. Shanmugavel [38] implemented the Clothoid method to generate safe and flyable flight paths for a cooperative group of UAVs tasked to arrive simultaneously on a target. Al Nuaimi [39] compared the differences between the Dubins and Clothoid. Simulations considered factors such trajectory tracking control laws under various flight conditions. Results found that the Dubins path yielded increased tracking errors due to the discontinuous changed in lateral command accelerations at the transition points between circular arcs and straight segments. Clothoid methods would also be a suitable option for this application. However, accuracy of a UAV in following a command path is not a considered factor in this application.

2.3.3 Path Planning Methods Comparisons

Roadmap methods are best suited for obstacle or collision avoidance path planning. Both the Voronoi diagram and Cell decomposition can be applied in a two dimensional space however cell decomposition can be easily expanded to three dimensions. Roadmap methods are also low complex calculation intensive and are much easier to implement. Pose-based methods are best suited when a desired path must traverse a set of waypoints or perform a specific task. Generating shortest paths between consecutive waypoints is also an advantage of these methods. However, pose-based methods require more complex

calculations which can result in longer computation times when compared to roadmap methods.

2.4 Literature Review Conclusions

The reviewed literature indicates that fixed wing aircraft are best to search multiple POIs as they can achieve long duration flight times. Multirotor helicopters are most useful to investigate the located TOI as they can VTOL which make them ideal to deploy a sensor pod to provide additional TOI surveillance.

Tasking algorithm literature indicates that GAs can be easily implemented to solve a variety of UAV mission tasking problems using a customizable fitness function. MILP methods can be applied as well but have shown to result in high computation times as the complexity of the problem increases. DA is best used to find the shortest path through a series of nodes which is not the focus of this work. A GA was selected for the mission planning application as they allow solutions to be evaluated by means of customizable fitness function. In addition, existing GA applications in literature can be used as a basis to generate initial mission plans while an additional fitness function can be developed to evaluate mission re-plan solutions.

Path planning literature suggests that Dubins arcs can allow fixed wing aircraft bank maneuvers to be simplified using constant radius arcs. Although the continuous curvature profile of the Clothoid method may generate paths more suited for UAV command

trajectories, this work is not concerned with the tracking accuracy of a UAVs commanded path. Discrete methods are best used in applications that involve obstacle or collision avoidance flight paths. Due to the simplified paths generated via Dubins arcs, a pose-based Dubins path planning method will be applied to model two dimensional fixed wing and quadcopter flight paths.

Chapter 3

Adaptive Mission Planner

In this chapter, a sample mission scenario is presented first followed by an envisioned adaptive mission planner which would be used to plan the mission scenario. Next, implementation of the selected GA for mission planning and Dubins for path planning is presented. Lastly, design of the adaptive mission planer using the selected mission planning and path planning algorithms is presented.

3.1 Envisioned Adaptive Mission Planning System

In order to present the design of the envisioned adaptive mission planner, a sample mission scenario is presented first. A set of POIs must be simultaneously surveyed to locate an unknown TOI which requires additional close surveillance. POIs in the search space require multiple overhead fly-by visitations and no two POIs can be visited simultaneously

within a specified window of time. Example of a search space containing nine POIs which are equally spaced apart in a three by three matrix configuration can be seen in Figure 3.1. The home base location is centered and away from the nine POIs and is where vehicles will deploy from and return to. TOI location is initially unknown but for illustration purposes the TOI is annotated as POI #5. Search space size is based off the flight distance range capabilities of a small hand launched UAV.

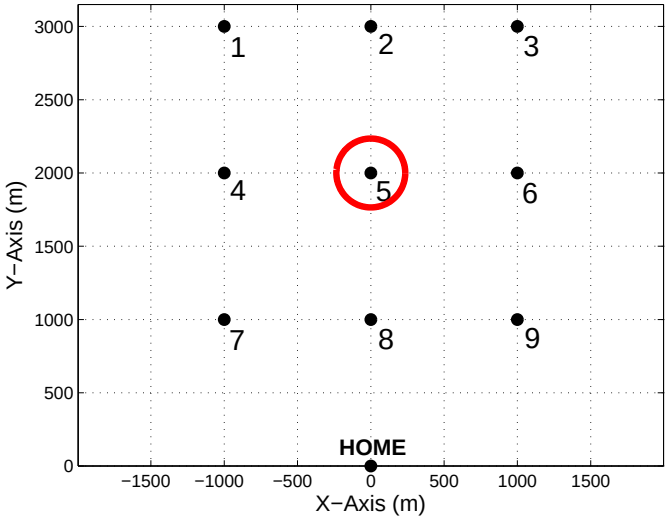

FIGURE 3.1: Scenario Search Space

First, an initial mission plan must be developed to task a fixed wing aircraft set, which are optimized for endurance, to survey POIs simultaneously in search of a TOI. Aircraft will be deployed from the same home base location and are assumed to be flying at varying altitudes to avoid aerial collisions. To maximize surveillance time, POI visitation loads will be evenly tasked amongst the fixed wing aircraft set. Once the TOI is located, a mission re-plan must be developed in which a vertical take off and landing vehicle, such a

quadcopter will be deployed from the home base location to visit the TOI. The quadcopter will fly at a low altitude so as to deploy a sensor pod at the TOI to obtain additional close surveillance. Additional POIs that have either been unvisited or still require visitations will also be tasked to the quadcopter. Remaining POIs not tasked to the quadcopter will then be evenly re-tasked amongst the fixed wing aircraft set. Once the TOI and remaining POIs have been visited, the fixed wing aircraft set and quadcopter will return to the home base location.

An envisioned adaptive mission planning system used to generate initial and mission re-plans can be seen in Figure 3.2. Systems of the adaptive mission planner included a GA based initial mission planning system and mission re-planning system. Mission planners are activated based on the mission and GA parameter inputs provided and a final initial or mission re-plan is outputted. In addition, a Dubins path planning algorithm will be built into the mission planners to simulate missions in order to evaluate the performance of the mission plan solutions. Implementation of the selected GA for mission planning and Dubins path planning for flight path simulation will now be presented in the proceeding sections.

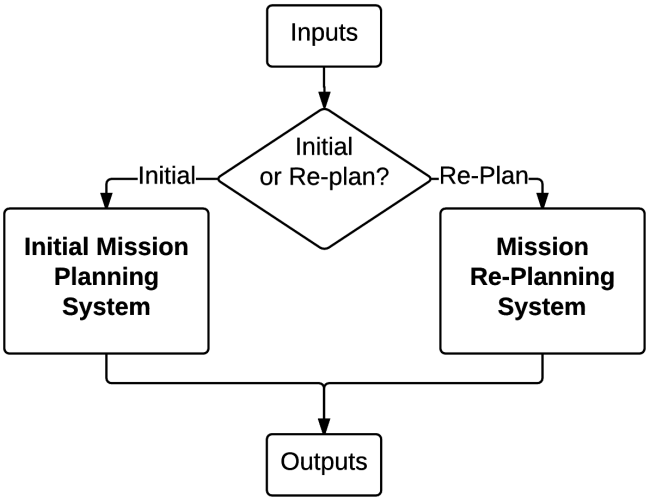

FIGURE 3.2: Envisioned Adaptive Mission Planner

3.2 Genetic Algorithm Mission Planning Implementation

GA implementation to generate mission plan solutions is presented in this section. First, the GA genetic representation used to characterize mission plan solutions is discussed. Next, selection/reproduction and genetic alteration operators are defined. Lastly, fitness functions designed to evaluate fixed wing and quadcopter mission plans is presented.

3.2.1 Genetic Representation

Real Representation (RR) was used to encode the chromosome parameters which meant that parameters were represented using real number vectors [25]. Chromosomes were expressed by 2 x L vectors, where L is the length of the chromosome. Vehicle numbers

are represented in the top row, which represent both fixed wing and quadcopter platforms, and POI numbers are represented in the bottom row. Tasking was then defined as the pair assignment between a top row vehicle number and a bottom row POI number. Priority parameters were assigned to POIs which determined the number of times the POI was to be visited during the mission. Summation of priority parameters determined the length, L, of the chromosome. Table 3.1 illustrates a sample chromosome using 5 POIs and 3 UAVs. POIs 1 & 2 were assigned a priority of 1, POIs 3 & 4 were assigned a priority of 2 and POI 5 a priority of 3.

1	3	1	2	3	2	1	2	3
2	1	5	5	3	4	4	3	5

TABLE 3.1: Sample Chromosome

3.2.2 Initial Population

An initial population size of 52 was selected based on a population convergence analysis performed on the GA used to task a homogeneous set of fixed wing aircraft in a balanced surveillance mission [25][26].

3.2.3 Selection/Reproduction

Roulette-wheel selection, augmented with elitist section, was used in this application. In this case, the roulette-wheel selection determined which chromosomes will engage with crossover alterations.

3.2.4 Genetic Alterations

Both crossover and mutation operators were implemented to perform alterations on chromosomes. Crossover was applied on even generations on the chromosomes selected by the roulette-wheel. Mutation was applied on odd generations.

3.2.4.1 Crossover

Crossover was applied at random chromosome partition locations. First, two chromosomes were selected as parents. Next, both chromosomes were split at the same partition and concatenated with each other to make two new children chromosomes.

3.2.4.2 Mutation

Mutation altered random elements in the current population. The number of elements randomly mutated in the population was determined by a mutation rate. Using the GA design that tasked a homogeneous set of fixed wing aircraft[25], a mutation rate of 21 was selected.

3.2.5 Fitness Evaluation

3.2.5.1 Initial Fixed Wing Fitness Function

Fixed wing aircraft were initially deployed to survey a set of POIs in search of a TOI. Since the TOI location was initially unknown, the initial GA mission planner was to develop a mission plan that balanced flight times and POI visitation loads amongst the fixed wing aircraft. Satisfying the following requirements from a previous GA application ensured that this mission was achieved [25]:

1. Maximize mission time to allow for maximum possible surveillance. Maximizing UAV surveillance times ensures that the term D is maximized.

2. Balance task loads evenly amongst UAVs in the set. Even distribution of POI task loads ensures that the term S is minimized.

3. UAVs must not reach a POI within too short of a time window which is represented by the N term.

Based off the previous requirements, the fixed wing fitness function can be seen in Equation 3.1

$$Fitness_{FWInitial} = \frac{D - S}{N + 1} \tag{3.1}$$

$D =$ Summation of all UAV flight times traveled

$S = d_{MAX} - d_{MIN}$ where d_{MAX} is the the maximum UAV flight time traveled and d_{MIN} is the minimum UAV flight time traveled

$N =$ The number of times in which two UAVs arrive at the same POI within a specified window of time

3.2.5.2 Re-plan Fixed Wing Fitness Function

Once a TOI was found in the search space, a quadcopter was to be deployed to visit the TOI. At this time, the fixed wing aircraft were re-tasked to continue visitations of unsearched POIs while the quadcopter visits the TOI and additional POIs. Re-tasking is achieved using a summation of the initial fixed wing fitness function and the additional term seen in Equation 3.2.

$$Fitness_{FW\,Additional} = \sum_{i=1}^{n} \frac{1}{FW_n} \tag{3.2}$$

$FW_n =$ Summation of all fixed wing aircraft flight times traveled to first assigned POI. Aircraft number is denoted by the term "n".

Adding this term ensured that during a mission re-plan the fixed wing aircraft set visit POIs closest to their current position in the space first. Since the flight time to the first assigned POI must be minimized, the reciprocal of this term was added to increase the fitness score. The re-plan fitness function can be seen in Equation 3.3 with each term carrying a weight of one.

$$Fitness_{FW\,Replan} = \frac{D - S}{N + 1} + \sum_{i=1}^{n} \frac{1}{FW_n} \tag{3.3}$$

In order to highlight the significance of the additional term, a sample UAV path scenario is presented. Three aircraft were assumed to travel similar triangular paths as seen in Figure 3.3. Aircraft deployed from the home base location and simultaneously visited points A and B before returning to the home base location. Aircraft paths were simplified using straight path segments and each aircraft traveled at a cruising speed of 15 meters/second. Aircraft flight times between path segments can be seen in Table 3.2.

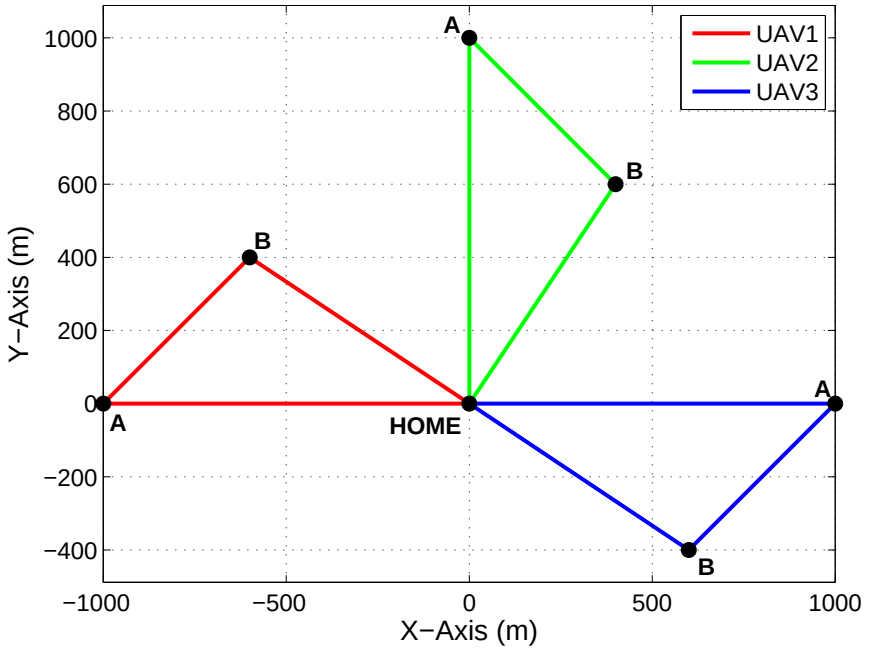

FIGURE 3.3: Triangular UAV Path

Path Segment	Home-A	A-B	B-Home
Aircraft Flight Time (min.)	1.11	0.63	0.80

TABLE 3.2: Aircraft Flight Times Between Path Segments

Potential aircraft visitation orders consisted of either visiting point A first or point B first. Fitness evaluation for the aircraft visitation orders were broken up into two parts, initial fixed wing fitness as seen in Equation 3.1 and the additional term as seen in Equation 3.2. Summation of these two equations equaled the final fitness value and can be seen in Table 3.3. Results indicated that the value of the additional term was larger when the aircraft set visited point B first. Inversely, when the aircraft set visited point A first, the value of the additional term was smaller. Reason for this behavior is that aircraft flight time to point B was shorter from the home base location when compared to point A as seen in Table 3.2.

Visitation Order	Equation 3.1 Initial Fixed Wing Fitness Value	Equation 3.2 Additional Fixed Wing Term Value	Equation 3.3 Re-plan Fixed Wing Fitness Value
Home-A-B-Home	7.62	2.70	10.32
Home-B-A-Home	7.62	3.74	11.37

TABLE 3.3: Aircraft Visitation Order Fitness Values

3.2.5.3 Quadcopter Fitness Function

When a TOI was found by the set of fixed wing aircraft, a quadcopter was deployed with the intention of visiting the TOI while alleviating the POI loads of the fixed wing aircraft. Alleviating the POI loads on the fixed wing aircraft was achieved by tasking the

quadcopter to visit the TOI while visiting additional unsearched POIs to and from the TOI. Satisfying the following requirements ensured that quadcopter mission objectives were achieved:

1. TOI must be visited and is represented by the term D_{TOI}
2. Visit additional POIs on route to and from TOI which is represented by the term $\frac{POI_{Visited}}{POI_{Total}}$
3. Maximize the battery usage by visiting as many additional POIs within the battery constraint which is represented by the term $(100 - Battery_{Mission})$

Based off the previous requirements, the quadcopter fitness function can be seen in Equations 3.4 and 3.5:

$$Fitness_{QR} = D_{TOI} * \frac{POI_{Visited}}{POI_{Total}} * (100 - Battery_{Mission}) \tag{3.4}$$

$$Battery_{Mission} = \frac{DistanceTraveled}{Distance_{FullBattery}} * 100 \tag{3.5}$$

$D_{TOI} =$ Reward for visiting the TOI ($D_{TOI} = 1$) and or penalty for failing to visit the TOI ($D_{TOI} = 0$)

$POI_{Visited} =$ Number of POIs visited by quadcopter

$POI_{Total} =$ Total number of POI visitations remaining

$DistanceTraveled =$ Distance traveled by quadcopter

$Distance_{FullBattery}$ = Total distance traveled on a full quadcopter battery

GA implementation to generate mission plan solutions has now been presented. Next, Dubins path planning implementation to simulate fixed wing and quadcopter flight plans will be presented.

3.3 Dubins Path Planning Implementation

3.3.1 2D Fixed Wing Aircraft Flight Path

Two dimensional fixed wing flight paths were generated using the Dubins paradigm [36]. Bank maneuvers were described using Dubins arcs and forward movement using Dubins straight paths. Fixed wing flight path was modeled based on the 3D Robotics Aero fixed wing aircraft[1] and can be seen in Figure 3.4. Aircraft parameters seen below are representative of the Aero aircraft specifications:

1. 15 meter/second cruise speed
2. 11 degree turn-rate angle per second
3. 77 meter turn radius
4. 30, 45 and 60 meter cruising altitudes

5. 30 minute flight time on full battery. Flight time was a selected percentage of the estimated 40 minute flight time by 3D Robotics to account for battery usage during take-off and landing.

FIGURE 3.4: 3DR Aero Fixed Wing Aircraft [1]

Using the vehicle parameters for the fixed wing aircraft, a simulation of the fixed wing aircraft flight path can be seen through a series of POIs in Figure 3.5.

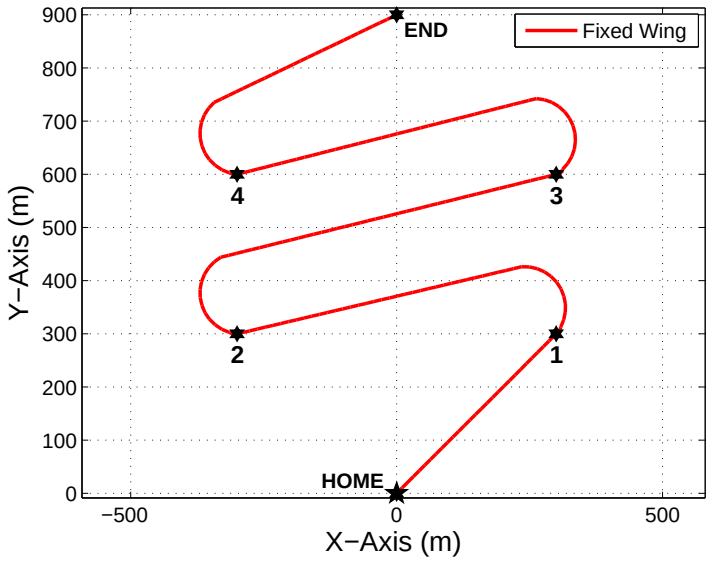

FIGURE 3.5: Fixed Wing Dubins Flight Path

3.3.2 2D Quadcopter Flight Path

Quadcopter flight path was generated using Dubins straight path segments between consecutive POIs. Straight path segments were used as the quadcopter was capable of changing direction at any moment. Quadcopter flight path was modeled after the 3D Robotic IRIS quadcopter [2] seen in Figure 3.6. Vehicle parameters seen below are representative of the IRIS quadcopter specifications:

1. 25 meter/second cruise speed

2. 5 meter cruising altitude

3. 10 minute flight time on full battery. Flight time was a selected percentage of the estimated 16-22 minute flight time by 3D Robotics to account battery usage during take-off and landing.

FIGURE 3.6: 3DR IRIS Quadcopter [2]

Using the vehicle parameters for the quadcopter, a simulation of the quadcopter flight path can be seen in Figure 3.7.

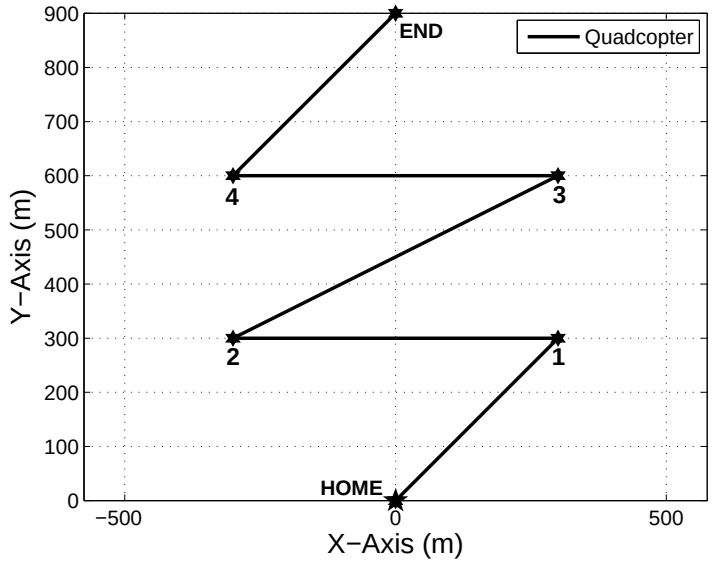

FIGURE 3.7: Quadcopter Trajectory

Implementation of the Dubins paradigm to generate two dimensional flight paths has now been presented. The designed adaptive mission planner using the GA for mission planning and Dubins path planning algorithm will be presented next.

3.4 Designed Adaptive Mission Planner

The developed adaptive mission planning system utilized two GAs to generate initial and mission re-plan solutions. Each GA mission planner was activated based on the mission and GA parameters provided to the adaptive mission planner. The final initial or mission re-plan was then outputted. Within each GA mission planner were several components which included the following: population, evaluation, convergence verification,

selection/reproduction and genetic alterations which can be seen in Figure 3.8. Mission and GA parameters provided were used to generate an initial random population of mission plan solutions. The evaluation system simulated mission flight paths using the Dubins path planning algorithm and evaluated the mission plans using the designed GA fitness functions. A GA convergence criterion was then checked to determine if the desired number of GA generations had been satisfied. If convergence was satisfied, then the final mission plan solution was outputted otherwise a new population of solutions was generated. Selection/reproduction operators, such as the roulette wheel method and elitist strategies, were applied to select best fit solutions within the current population of solutions. Genetic alterations, such as crossover and mutation operators, then modified the selected population to produce a new current population of mission plan solutions. GA generations continued until the convergence criterion was satisfied. Inputs of the initial GA mission planning system will be presented next followed by those of the GA mission re-planning system.

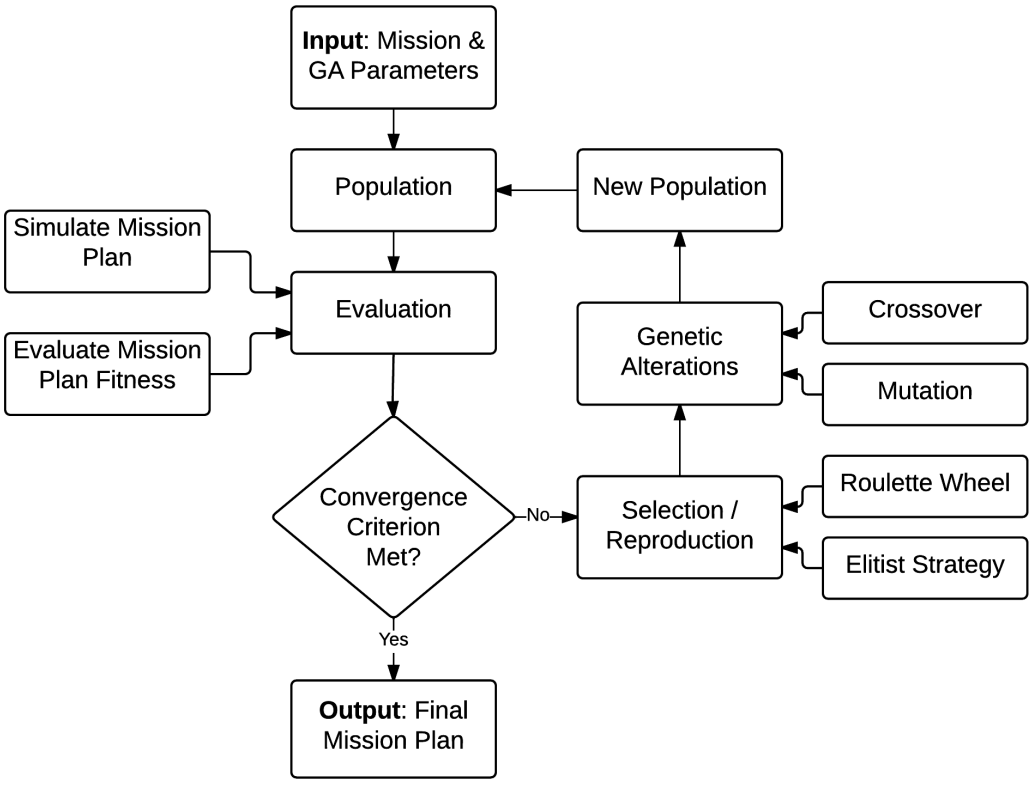

FIGURE 3.8: GA Initial Mission Planner and Re-Planner Components

3.4.1 GA Initial Mission Planner

Initial GA mission planning was activated during the initial search of the POIs. Fixed wing aircraft in the set were assigned to visit a balanced number of POIs. Initial mission and GA parameter inputs include the following:

- Home base coordinates
- POI coordinates and frequency of visitation
- Number of fixed wing aircraft

- POI visitation window time constraint
- GA parameters which include: population size, chromosome structure and number of desired generations

Evaluation in the initial mission planner consisted of simulating the fixed wing flight paths and evaluating the fitness value of the mission plans. Once the GA completed the desired number of generations, the final initial mission plan was outputted.

3.4.2 GA Mission Re-Planner

GA mission re-planning was activated once the TOI had been located by one of the fixed wing aircraft. At this time, a quadcopter was deployed to visit the TOI and additional unsearched POIs. Remaining unsearched POIs were then re-tasked amongst the fixed wing aircraft set. Mission re-plan and GA parameter inputs included the following:

- Home base coordinates
- TOI coordinate location
- Unsearched POI coordinates and remaining frequency of visitation
- POI visitation window time constraint
- Fixed wing aircraft vehicle states which includes the current coordinate location and remaining battery life

- GA parameters which include: population size, chromosome structure and number of desired generations

Evaluation in the re-plan GA consisted of simulating mission plans and evaluating fitness values for both quadcopter and fixed wing vehicles. Mission plans contained unsearched POIs and the TOI. The quadcopter mission plan was simulated first and remaining POIs not visited by the quadcopter were simulated in a separate mission plan using fixed wing aircraft set. Quadcopter and fixed wing mission plans were then evaluated, using the designed fitness functions, to determine individual vehicle set fitness values. Summation of the two fitness values then equaled the overall mission plan fitness value. Once the re-plan GA completed the desired number of generations, the final mission re-plan was outputted. Simulations of the adaptive mission planner are presented in the next chapter to ensure that the designed systems satisfied initial and mission re-planning objectives.

Chapter 4

Mission Planning Simulations

4.1 Simulation Overview

Simulations of the initial and mission re-planning systems are presented in this chapter. First, the initial GA mission planning system was simulated to ensure that POI task loads were balanced amongst the fixed wing aircraft. Second, the re-plan GA mission planning system was simulated to ensure that the TOI was visited by the deployed quadcopter and remaining POIs were evenly redistributed amongst the fixed wing aircraft set. Next, both the initial and re-plan GA mission planning systems were simulated together to test the effectiveness of the adaptive mission planner. Lastly, case studies were simulated in which the number of fixed wing aircraft in the heterogeneous UAV sets varied along with the location of a single TOI. All search space sizes used in the simulations were based off a small fixed wing aircraft and quadcopter flight distance ranges.

4.2 Initial GA Simulation

Initial GA mission planning consisted of the initial fixed wing aircraft fitness function and the fixed wing aircraft flight path planner. It was required that the obtained mission plan solution balance the flight times and POI visitation loads amongst the fixed wing aircraft in the set. Initial GA mission planning was simulated by selecting a scenario in which a set of fixed wing aircrafts were required to fly over a series of POIs. Mission and GA parameters used to simulated the mission can be seen below and the search space can be seen in Figure 4.1:

1. 1200m x 900m Search Space
2. 5 POIs with Priority 3
3. 3 Fixed Wing Aircraft
4. Delta = 0.50 min. (30 Second Window)
5. GA Generations = 350

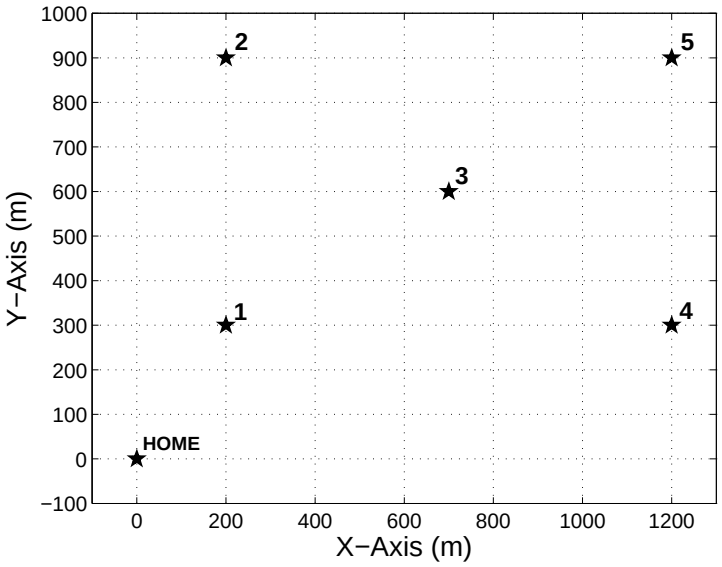

FIGURE 4.1: Initial Search Space

After 350 GA generations, the best initial chromosome obtained based on fitness function score can be seen in Table 4.1. As seen in the chromosome, All fixed wing aircrafts were tasked to visit 5 POIs each thus satisfying the mission requirement of balancing the POI task loads.

1	2	1	3	2	1	2	3	3	3	1	3	2	1	2
5	1	3	3	2	5	4	1	4	2	1	4	2	3	5

TABLE 4.1: Initial Best Chromosome

Fixed wing flight times and distances traveled can be seen in Table 4.2. Since POI visitation loads were evenly distributed amongst the fixed wing aircraft, an average mission time of 7.3 minutes was obtained. Flight path trajectories for the initial mission plan solution can then be seen in Figure 4.2.

	Fixed Wing 1	Fixed Wing 2	Fixed Wing 3	Avg	Std Dev
Flight Time (min.)	7.2	7.1	7.7	7.3	0.3
Flight Distance (m.)	6522.8	6464.6	6978.1	6645.2	291.7

TABLE 4.2: Initial Flight Times & Distances

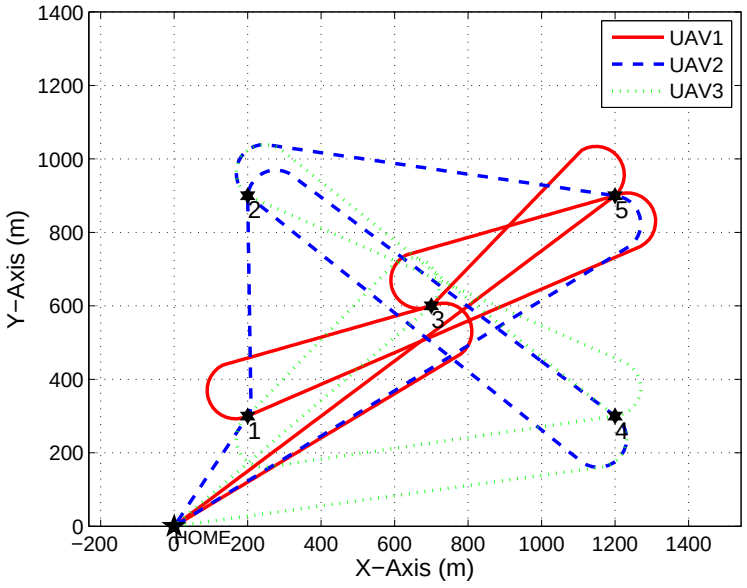

FIGURE 4.2: Initial Trajectory

In addition to ensuring that POI and flight times were balanced, no two aircraft were to reach the same POI within a 30 second time interval. Figure 4.3 illustrates the time in which a UAV arrives at a POI. It can be seen that the smallest interval of time in which two UAVs arrive at a POI was 0.74 minutes, 39 seconds, at POI number 2.

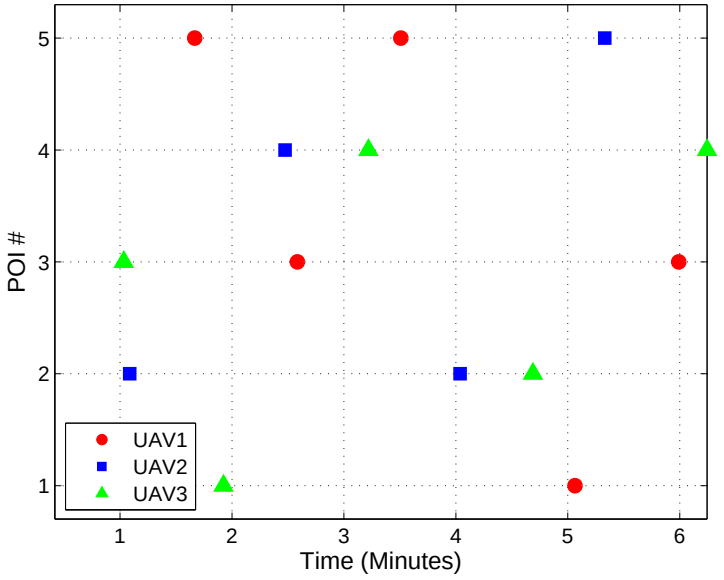

FIGURE 4.3: Initial POI Timeline

GA run time and convergence during the initial mission plan can be seen in Table 4.3 and the fitness scores vs generations in Figure 4.4. In order to complete 350 generations the GA ran for total of 4.8 minutes resulting in a final fitness score of 25.6. Delta G represents the number of generations without an increase in fitness and in this scenario the fitness did not increase for 183 generations.

Run Time	Seconds/Generation	Convergence Time	Convergence Generation	ΔG
4.8 min.	0.8	132.8 sec.	169	183

TABLE 4.3: Initial GA Performance

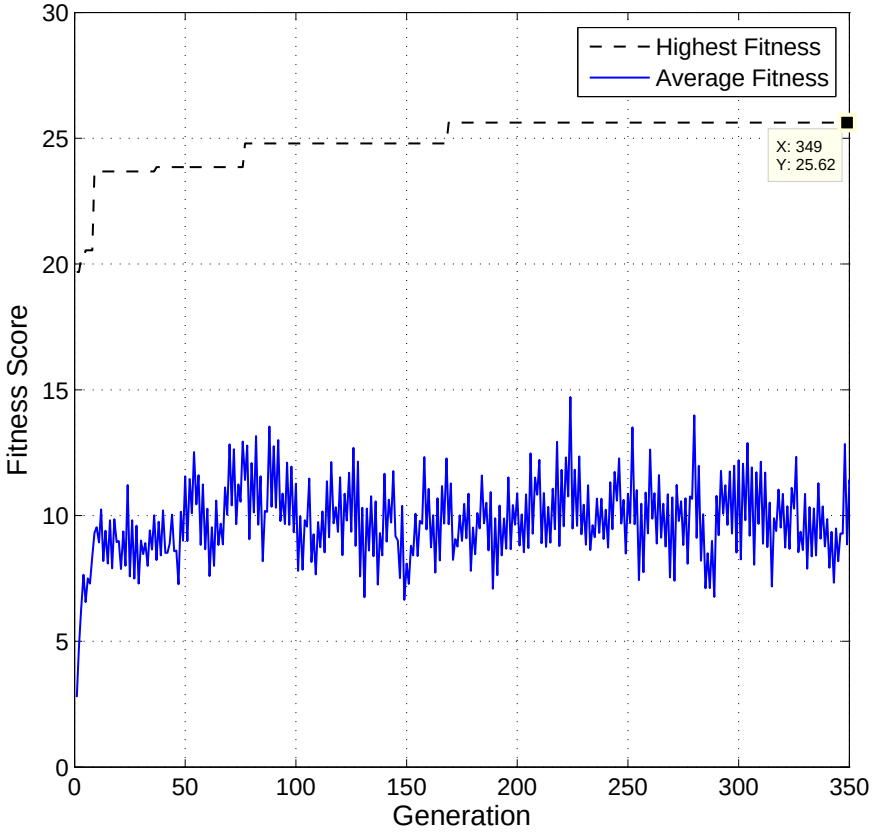

FIGURE 4.4: Initial Fitness vs Generations

4.3 Re-Plan GA Simulation

Once a TOI is found, the re-plan GA mission planner is activated. A quadcopter platform would to be deployed with the intention of visiting the TOI and additional POIs along its route to and from the TOI. Remaining POIs that have not yet been visited, or will not be visited by the quadcopter, were to be evenly redistributed amongst the fixed wing aircraft set. In order to achieve these mission objectives, the re-plan GA used a combination of the re-plan fixed wing and quadcopter fitness functions as well as their

flight path planners. In the event of a mission re-plan, the fixed wing aircraft will start from their current locations in the search space while the quadcopter is deployed from the home base location. However, to illustrate the effectiveness of the re-plan GA all vehicles began and ended at the home base location with POI #5 being a preselected TOI. Mission re-plan and GA parameters used to simulate the mission can be seen below and the search space in Figure 4.5.

1. 2000m x 3000m Search Space
2. 9 POIs with Priority 1
3. 3 Fixed Wing Aircraft + 1 Quadcotper
4. Target of Interest (TOI) = 5
5. Delta = 0.50 min. (30 Second Window)
6. GA Generations = 350

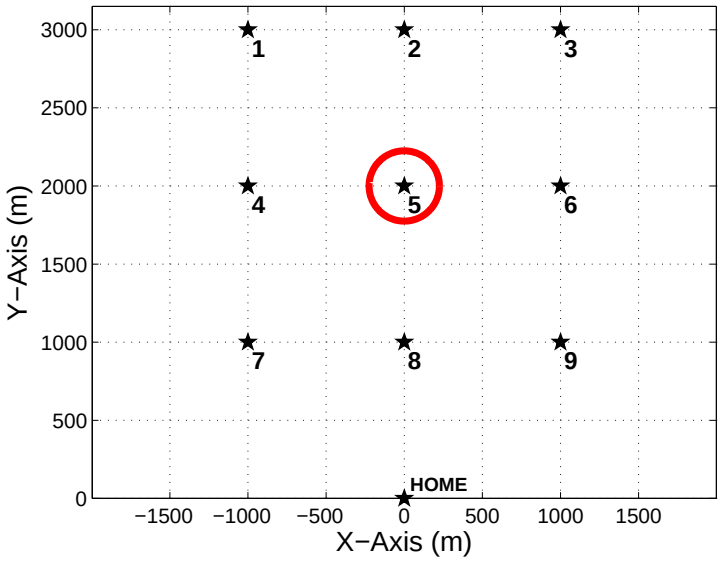

FIGURE 4.5: Re-Plan Search Space

After 350 GA generations, the best initial chromosome obtained based on fitness function score can be seen in Table 4.4. It can be seen that each fixed wing aircraft was tasked to visit two POIs while the quadcopter was tasked to not only visit the TOI but two additional POIs.

4	2	1	3	1	4	3	2	4
7	9	4	6	3	5	1	2	8

TABLE 4.4: Re-Plan Best Chromosome

Vehicle flight times and distances can then be seen in Table 4.5. Fixed wing flight times were balanced while the quadcopter traveled for 3.2 minutes and ended with 68 % of its battery life remaining. Figure 4.6 then illustrates the final re-plan trajectory.

	FW #1	FW #2	FW #3	Quadcotper	Avg	Std Dev
Flight Time (min.)	8.6	7.6	8.6	3.2	7.1	2.6
Flight Distance (m.)	7797.1	6835.2	7797.1	4860.7	6822.5	1384.2

TABLE 4.5: Re-Plan Flight Times and Distances

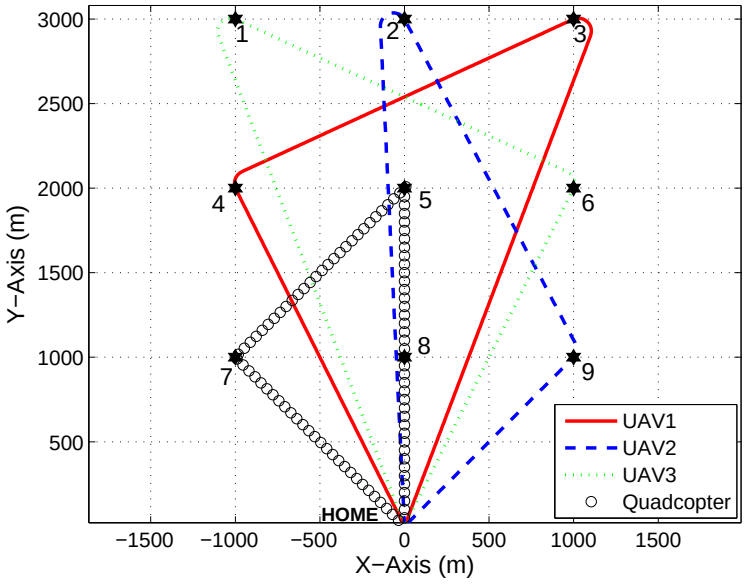

FIGURE 4.6: Re-Plan Trajectory

Similar to the in the initial mission plan, no two fixed wing aircraft were to reach the same POI within the 30 seconds time interval. However, since each POI was only given a priority level of one, no two aircraft reached the same POI during the simulation. Figure 4.7 illustrates the POI timeline of the re-plan mission.

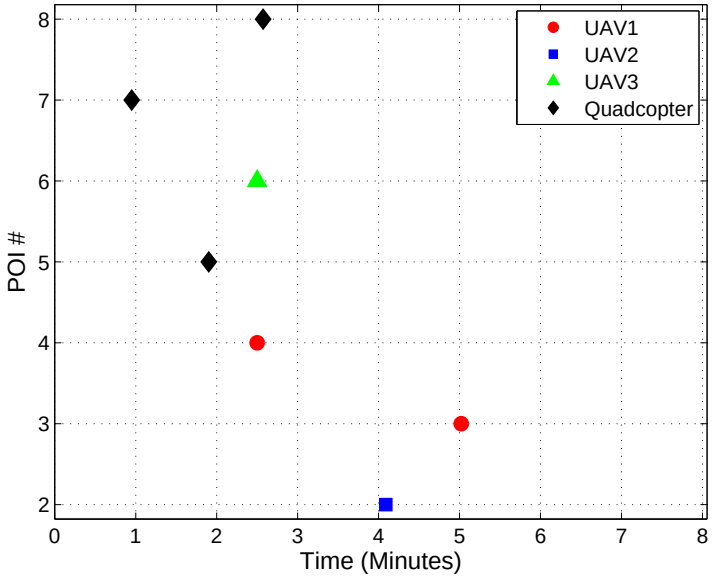

FIGURE 4.7: Re-Plan POI Timeline

GA run time and convergence performance of the mission re-plan can be seen in Table 4.6 and the fitness scores vs generations can be seen in Figure 4.8. In order to complete 350 generations, the re-plan GA ran for 5.3 minutes and attained its highest fitness score after 58 generations. At this generation, the fixed wing aircraft fitness score was 25.2 and the quadcopter was 15 for a total final fitness of 40.2. Average population fitness vs generations can then be seen in Figure 4.9. Results of this simulation indicated that the re-plan GA was capable of satisfying re-plan objectives.

Run Time	Seconds/Generation	Convergence Time	Convergence Generation	ΔG
5.3 min.	0.9	53.2 sec.	58	294

TABLE 4.6: Re-Plan GA Performance

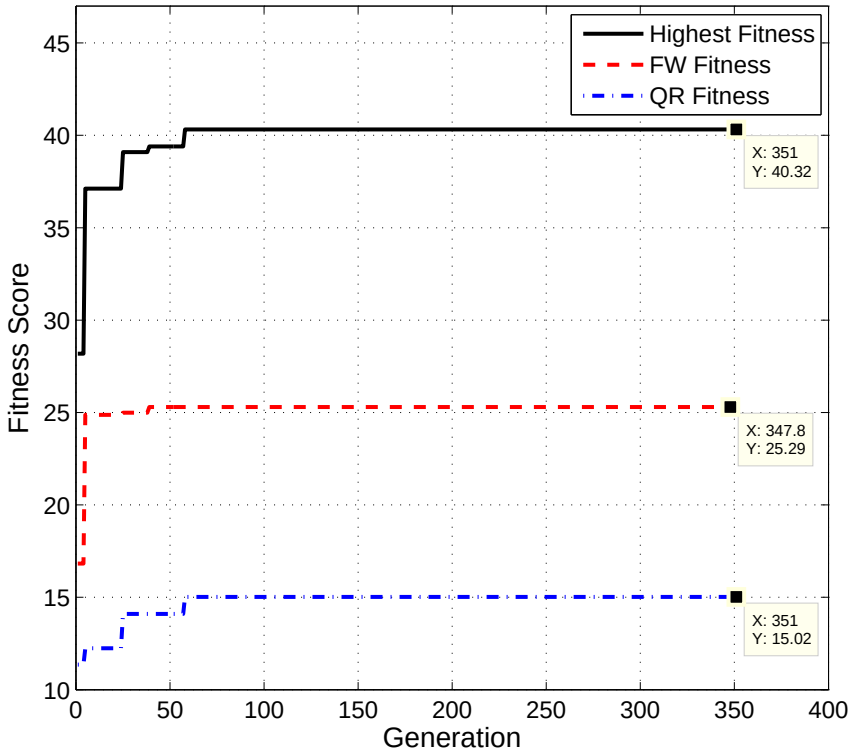

FIGURE 4.8: Re-Plan Fitness vs Generations

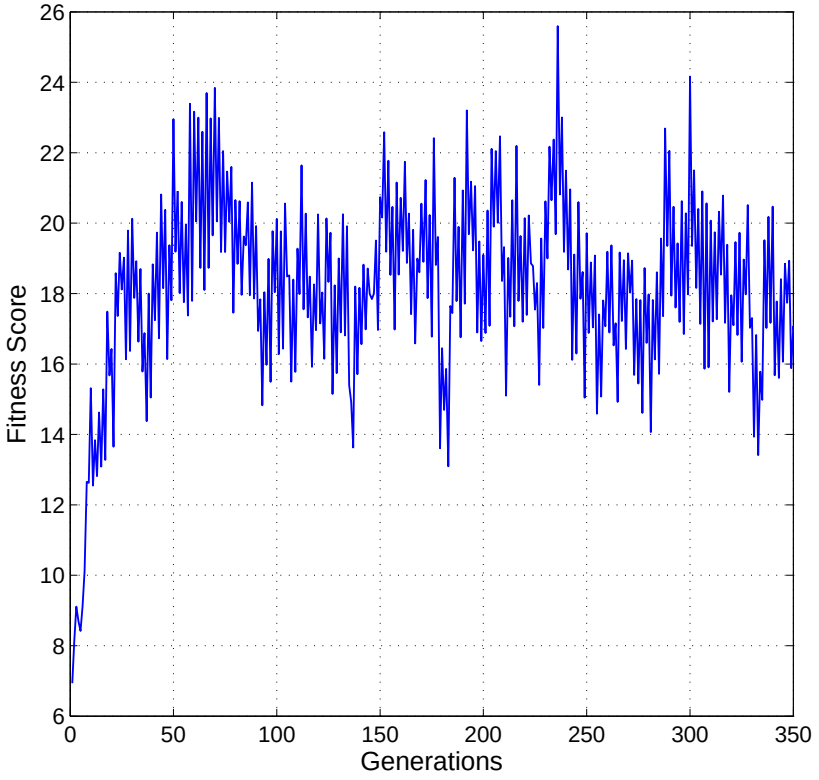

FIGURE 4.9: Re-Plan Average Population Fitness vs Generations

4.4 Adaptive Mission Planner Simulation

Initial and re-plan GAs were found to obtain missions that satisfied initial and re-plan objectives. Effectiveness of the combined systems in the adaptive mission planner was then tested by simulating a mission scenario. The procedure used to perform the adaptive mission planner simulation can be seen below and a flowchart illustrating the procedure in Figure 4.10.

1. Establish POI and search space
2. Run initial GA mission planner
3. Simulate initial mission plan until a preselected TOI is reached
4. Extract fixed wing vehicle states for mission re-plan
5. Run re-plan GA mission planner
6. Evaluate mission times as metric

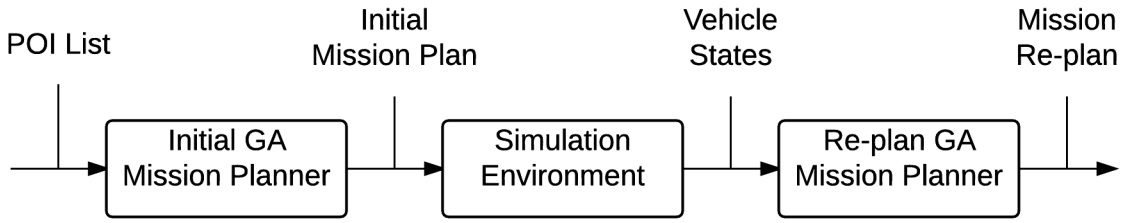

FIGURE 4.10: Adaptive Mission Planner Flowchart

Prior to conducting an adaptive mission planner simulation, a metric to quantifying the reductions in mission times by deployment of a quadcopter was developed. Both

reductions in fixed wing and overall mission times were examined and can be seen in Equations 4.1 and 4.2.

$$FixedWing_{Reduction} = 100 - \frac{\sum FW_{TimeTraveled} + \sum FW_{Re-PlanTime}}{\sum FW_{InitialTime}} * 100 \tag{4.1}$$

$$MissionTime_{Reduction} = 100 - \frac{\sum FW_{TimeTraveled} + \sum FW_{Re-PlanTime} + QR_{Time}}{\sum FW_{InitialTime}} * 100 \tag{4.2}$$

where

$\sum FW_{InitialTime}$ = Total initial mission time between all fixed wing aircraft

$\sum FW_{TimeTraveled}$ = Total mission time traveled between all fixed wing aircraft prior to locating TOI

$\sum FW_{Re-PlanTime}$ = Total re-plan mission time between all fixed wing aircraft

QR_{Time} = Total mission time of quadcopter

An adaptive mission planner simulation was conducted using the following initial parameters and the initial search space can be seen in Figure 4.11:

1. 1500m x 1000m Search Space
2. 9 POIs with Priority 2

3. 3 Fixed Wing Aircraft + 1 Quadcotper

4. Target of Interest (TOI) = 5

5. Delta = 0.50 min. (30 Second Window)

6. GA Generations = 350

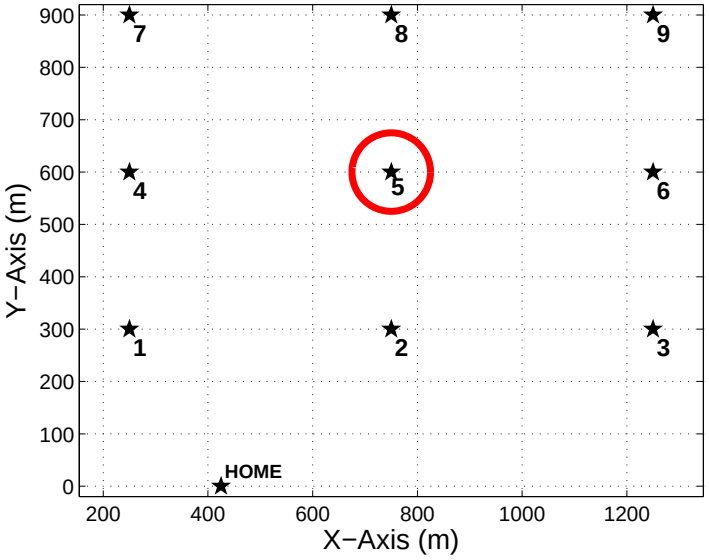

FIGURE 4.11: Adaptive Mission Planner Simulation Search Space

After 350 generations, the best initial GA mission planner chromosome seen in Table 4.7. POI visitation loads were balanced amongst the fixed wing aircraft as each were tasked to visit 6 POI. Figure 4.12 then shows the initial fixed wing aircraft trajectory.

3	3	2	3	2	1	3	2	1	3	3	2	2	1	1	2	1	1
6	8	1	2	5	2	7	7	3	3	5	9	1	4	6	9	4	8

TABLE 4.7: Adaptive Mission Planner Initial Best Chromosome

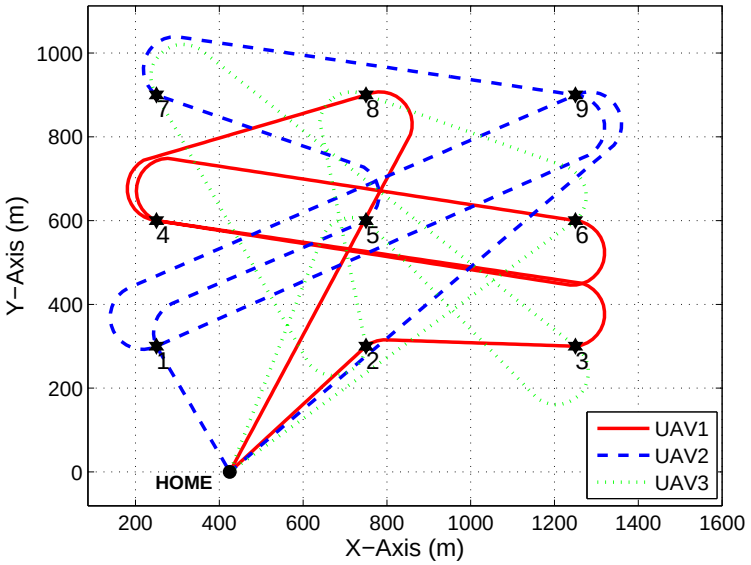

FIGURE 4.12: Scenario Initial Trajectory

POI #5 was assigned to be the TOI and further examination of the initial chromosome indicated that fixed wing aircraft #2 was assigned to first visit POI #1 followed by POI #5. This meant that fixed wing aircraft #1 & #3 will visit as many POIs in their mission plan before fixed wing aircraft #2 reaches the TOI. Figure 4.13 illustrates a simulation of the initial mission plan. It can be seen that fixed wing aircraft #1 reached POIs #2 & #3 and fixed wing #3 was inbound to POI #6 before the TOI was reached.

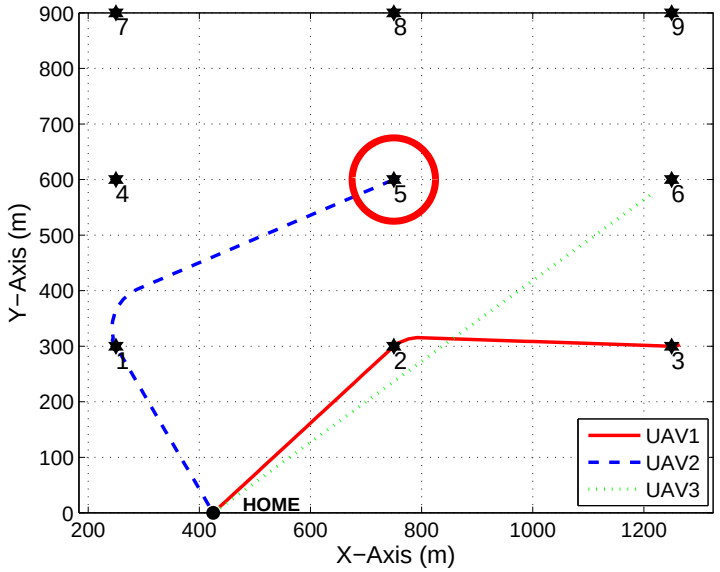

FIGURE 4.13: Adaptive Mission Planner Initial Mission Simulation

Current vehicle states of the fixed wing aircraft were then used to generate a mission re-plan and the best re-plan chromosome attained after 350 GA generations can be seen in Table 4.8. Upon further examination of the re-plan chromosome, the quadcopter was assigned to visit a total of 7 POIs including TOI #5. Fixed wing aircraft #1 & #3 were assigned to visit two POIs while fixed wing aircraft #2 was assigned to visit three remaining POIs. Re-plan trajectory can be seen illustrated in Figure 4.14.

3	4	1	4	2	2	2	4	4	4	1	4	3	4
6	2	3	6	8	9	1	9	8	5	7	7	4	4

TABLE 4.8: Adaptive Mission Planner Re-Plan Best Chromosome

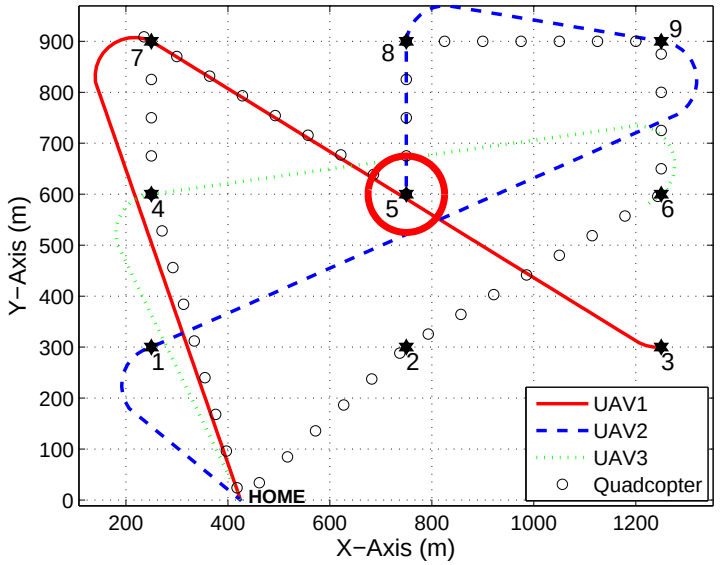

FIGURE 4.14: Adaptive Mission Planner Re-Plan Trajectory

Initial and re-plan flight distances and times can be seen in Tables 4.10 and 4.9. Flight distances and times were balanced in the initial mission plan which was expected as POI loads were balanced amongst the fixed wing aircraft. During the re-plan, fixed wing aircraft distances and times were also balanced while the quadcopter traveled for a total time of 2.7 minutes.

	FW #1	FW #2	FW #3	Quadcotper	Avg	Std Dev
Initial Flight Time (min.)	7.6	8.2	7.8		7.7	0.4
Re-Plan Flight Time (min.)	3.9	3.9	3.6	2.7	3.5	0.6

TABLE 4.9: Adaptive Mission Planner Flight Times

	FW #1	FW #2	FW #3	Quadcotper
Initial Flight Distance (m.)	6461.8	6955.3	6224.2	
Re-Plan Flight Distance (m.)	3489.9	3554.7	3239.4	4094.7

TABLE 4.10: Adaptive Mission Planner Flight Distances

GA performance for both the initial and re-plan solutions can be seen in Table 4.11. 350 GA generations in the initial mission plan ran for 4.8 minutes while the re-plan mission plan ran for 2.6 minutes. Fitness scores vs generations for both the initial and mission re-plan can be seen in Figures 4.15 and 4.16.

	Run Time	Sec/Gen	Convergence Time	Convergence Generation	ΔG
Initial	4.8 min.	0.8	153.4 sec.	183	169
Re-Plan	2.6 min.	0.5	143.7 sec.	310	42

TABLE 4.11: Adaptive Mission Planner GA Performances

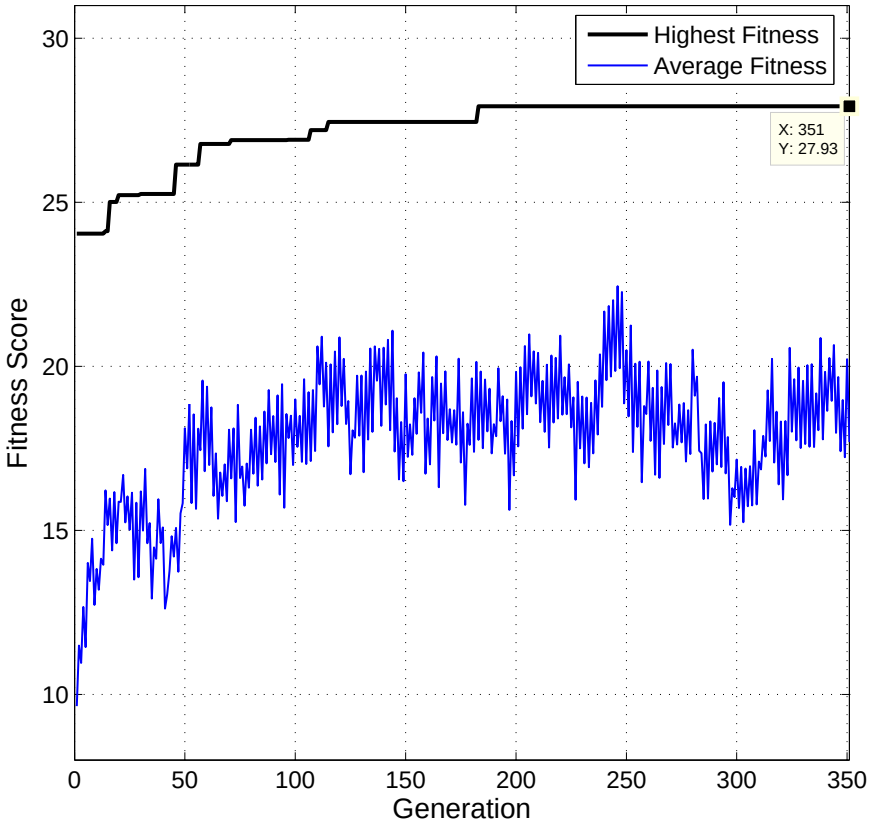

FIGURE 4.15: Adaptive Mission Planner Initial Fitness

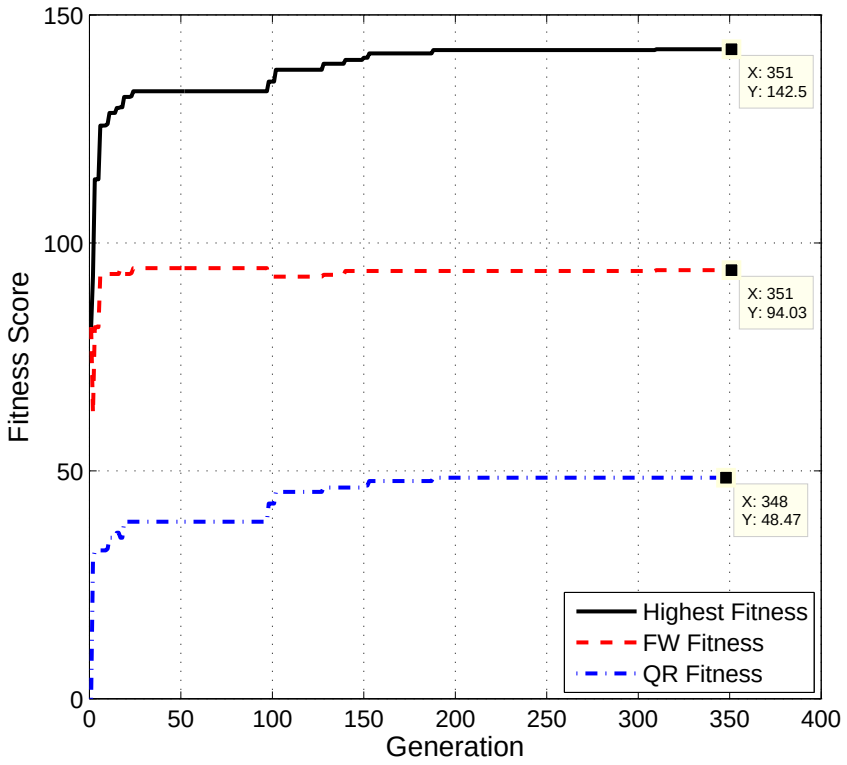

FIGURE 4.16: Adaptive Mission Planner Re-plan Fitness

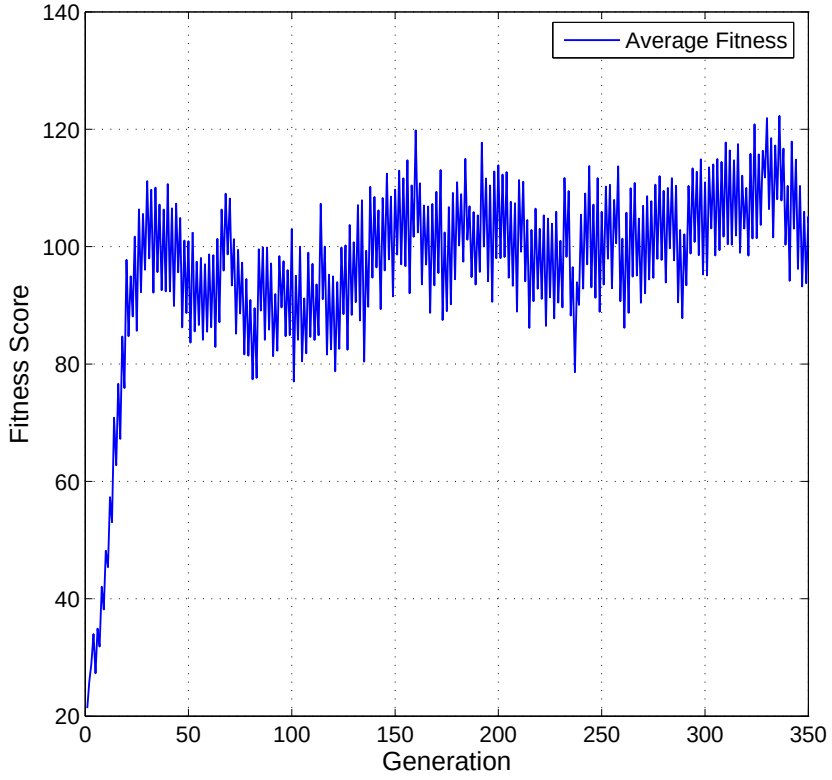

FIGURE 4.17: Average Population Fitness vs Generations

POI timelines for both the initial and re-plan mission can be seen in Figures 4.18 & 4.19. In the initial mission plan no two aircraft arrived at the same POI within the 30 second allowable window. Mission re-plan POI timeline indicated that no two fixed wing aircraft arrived at the same POI within the allowable 30 second window as well.

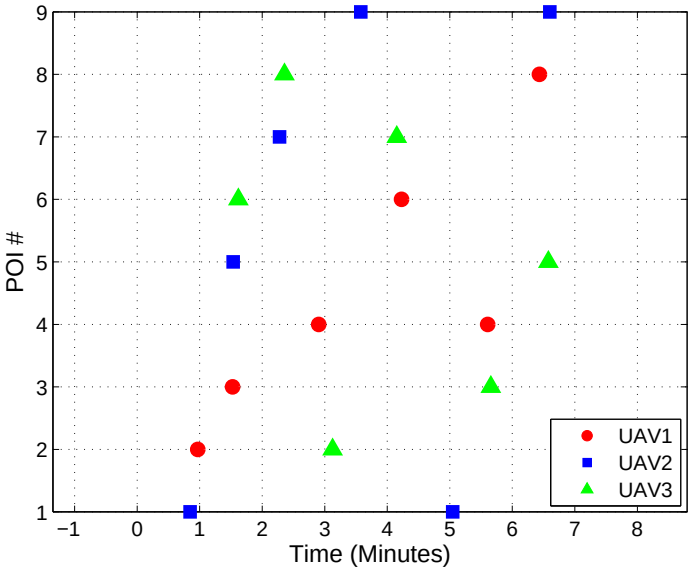

FIGURE 4.18: Adaptive Mission Planner Initial POI Timeline

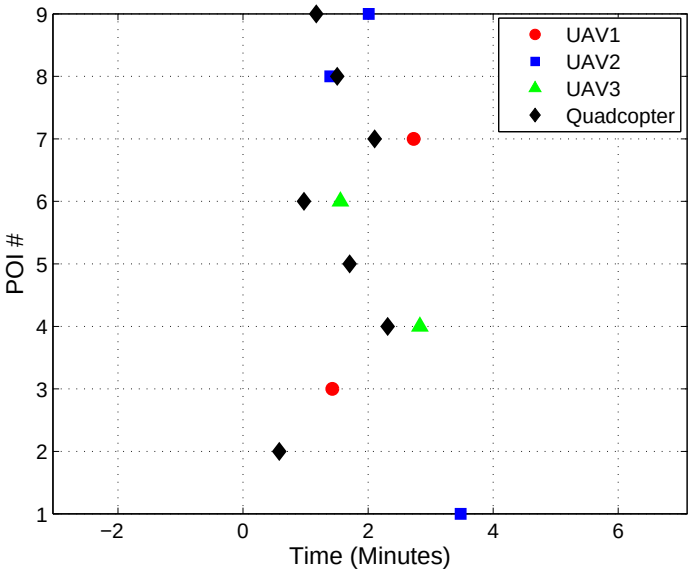

FIGURE 4.19: Adaptive Mission Planner Re-Plan POI Timeline

Simulation of the adaptive mission planner has now illustrated that initial and mission re-plan objectives are achieved. Reductions in fixed wing and overall mission times by the deployment of the quadcopter were then examined and can be seen in Table 4.12. Fixed wing aircraft mission times saw a reduction of 31% and the overall mission time was reduced by 19%. This reduction resulted in the entire mission being completed 18.7 minutes in comparison to the initial 23.2 minutes. To further expand on these simulation results, case studies were simulation where the number of UAVs in the heterogeneous sets varied.

Initial Fixed Wing Time (min.)	Simulation Time Traveled (min.)	Re-Plan Fixed Wing Time (min.)	Fixed Wing Time Reduction	Mission Time Reduction w/ Quadcopter
23.2	4.6	11.4	30.9 %	19.2 %

TABLE 4.12: Adaptive Mission Planner Metric Evaluation

4.5 Varying Vehicle Set Simulations

Adaptive mission planner case studies were simulated by varying the number of the fixed wing aircraft in the heterogeneous between 2,3 and 4 aircraft with one quadcopter. POIs in the search space were organized in a square formation with each POI requiring three visits as seen in Figure 4.20. In every vehicles set, a single TOI was rotated between one of the nine POIs. Simulations were conducted using the following GA parameters:

1. 1500m x 1000m Search Space

2. 9 POIs with Priority 3

3. 2,3 & 4 Fixed Wing Aircraft + 1 Quadcotper

4. Target of Interest (TOI) = 1-9

5. Delta = 0.50 min. (30 Second Window)

6. GA Generations = 350

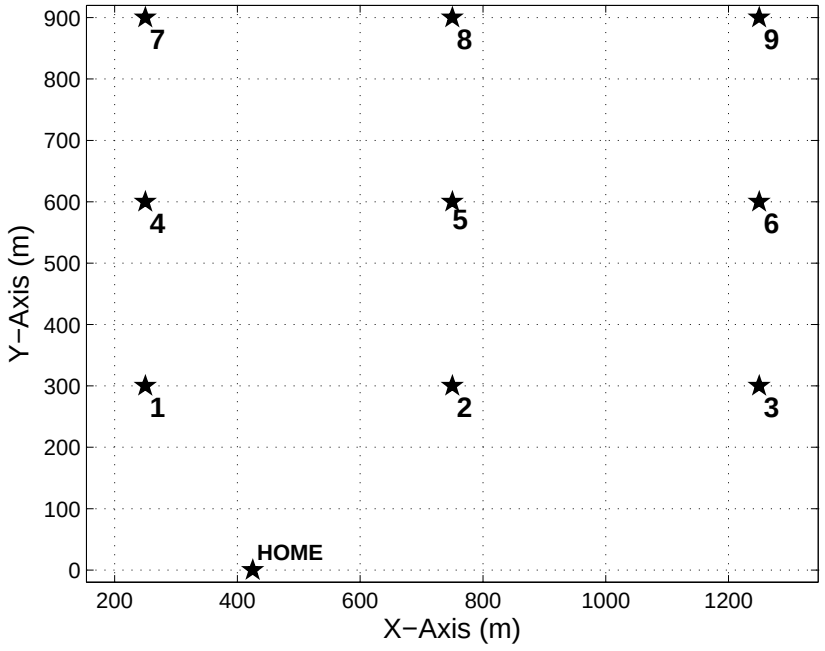

FIGURE 4.20: Varying Vehicle Search Space

Fixed wing aircraft mission time reductions can be seen in Figure 4.21 where each data set represented a heterogeneous UAV set containing either two, three or four fixed wing

aircraft and a single quadcopter. Results indicated that for these particular case studies, an average fixed wing mission time reduction of 42% was obtained when the heterogeneous set contained two fixed wing aircraft. Sets containing three fixed wing aircraft resulted in a 20% average mission time reduction while four fixed wing aircraft resulted in a 21% average mission time reduction.

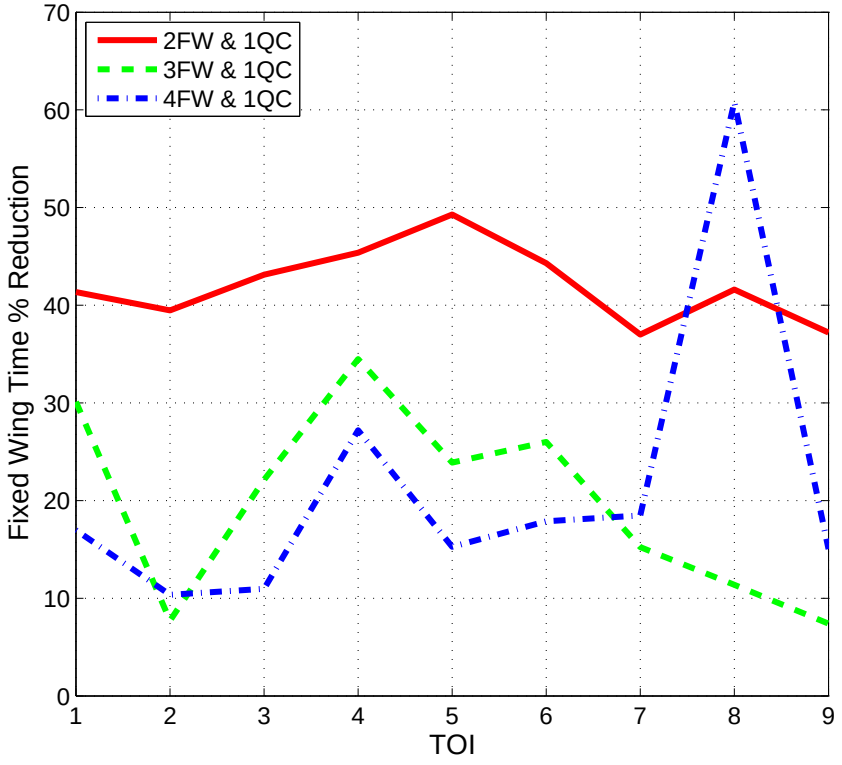

FIGURE 4.21: Case Study Fixed Wing Time Reductions

Overall mission time reductions can be seen in Figure 4.22. Simulation results of the previously mentioned case studies indicated average overall mission time reductions of 30% using two fixed wing aircraft, 11% using three fixed wing aircraft and 7% using four fixed wing aircraft.

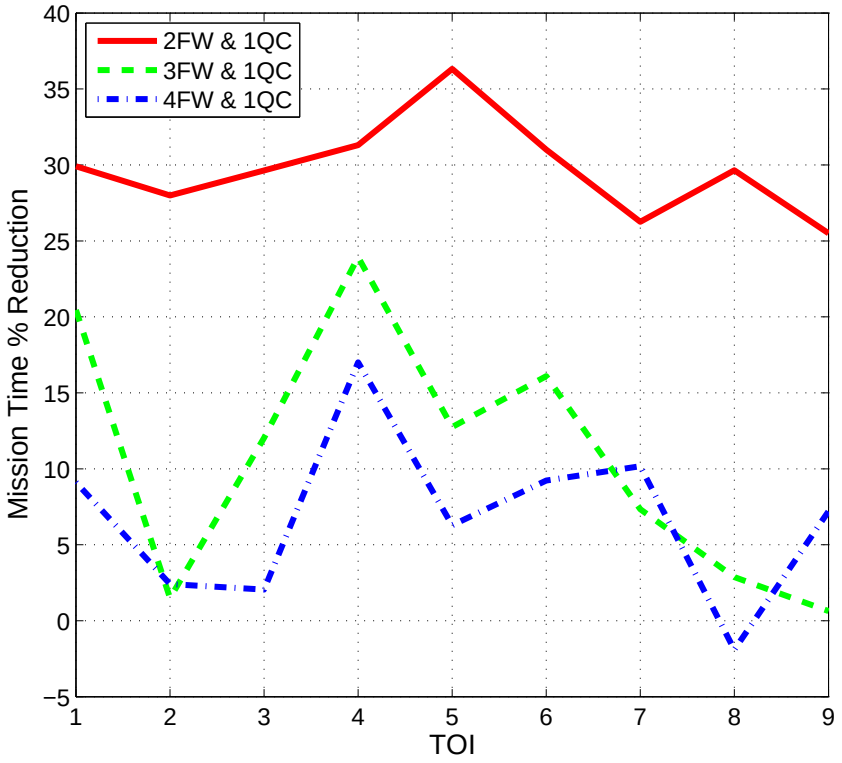

FIGURE 4.22: Case Study Mission Time Reductions

Quadcopter battery life remaining after each simulation can be seen in Figure 4.23. Results indicated that the quadcopter returned with and average remaining battery of 45% when two fixed wing aircraft were used in the heterogeneous set. Three fixed wing aircraft in the set resulted in a 69% average remaining battery and four fixed wing aircraft in the set resulted in a 70% average remaining battery.

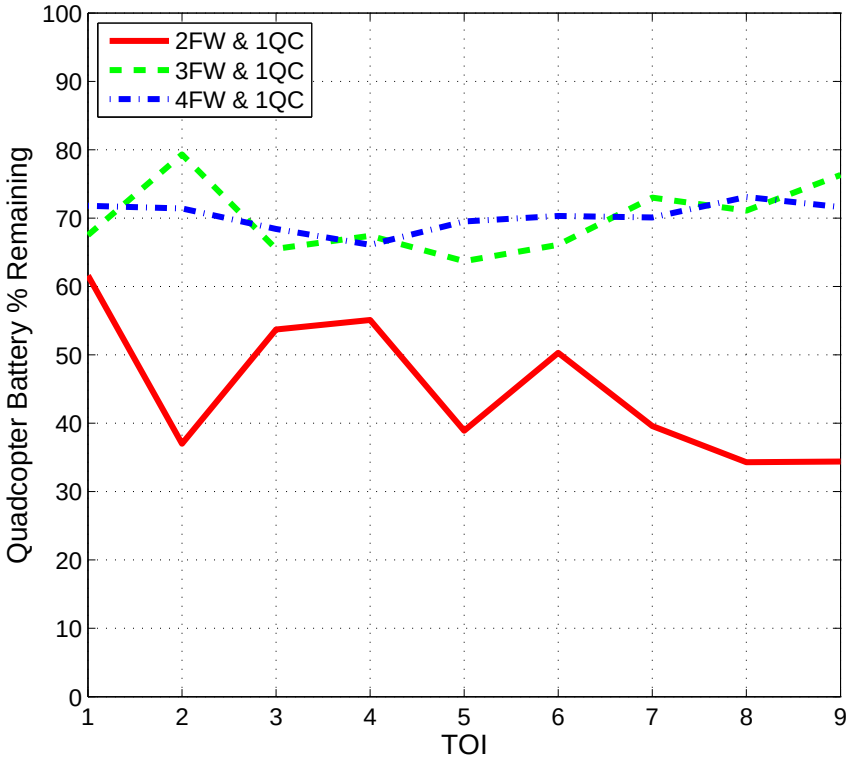

FIGURE 4.23: Case Study Quadcopter Battery Remaining

GA run times for the initial and mission re-plan can be seen in Figures 4.24 and 4.25. Average run times for the GA initial and mission re-plan can also be seen in Table 4.13. Results indicated that GA run times were greatest in both the initial and mission re-plan when two fixed wing aircraft were used. As the number of fixed wing aircraft increased, average GA run times decreased.

	2 Fixed Wing Aircraft	3 Fixed Wing Aircraft	4 Fixed Wing Aircraft
Initial Run Time (min.)	10.9	9.1	8.2
Re-Plan Run Time (min.)	4.1	3.8	4.7

TABLE 4.13: Average Case Studies GA Run Times

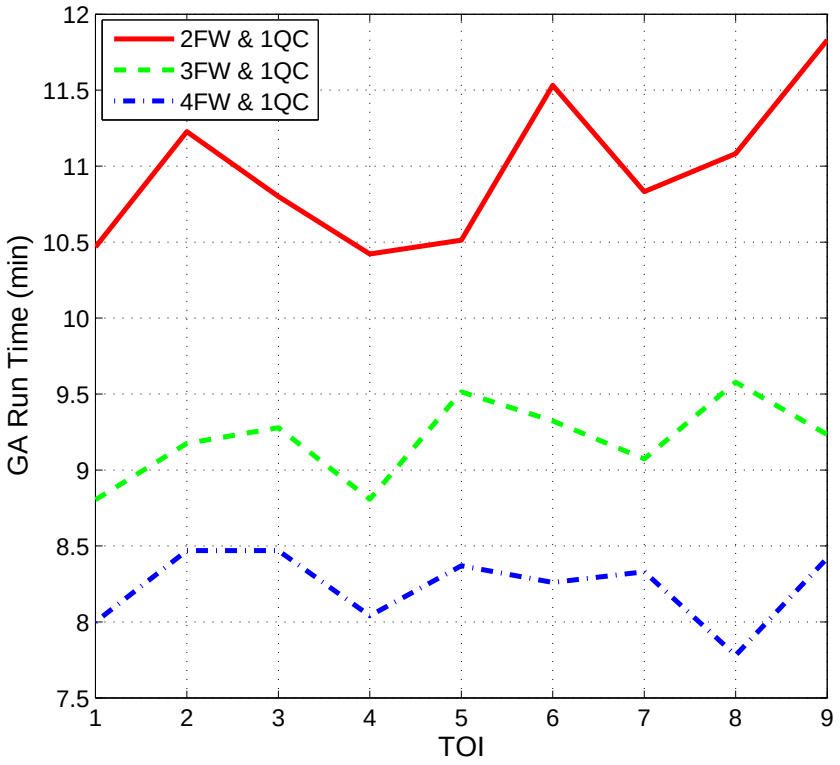

FIGURE 4.24: GA Initial Mission Plan Run Times

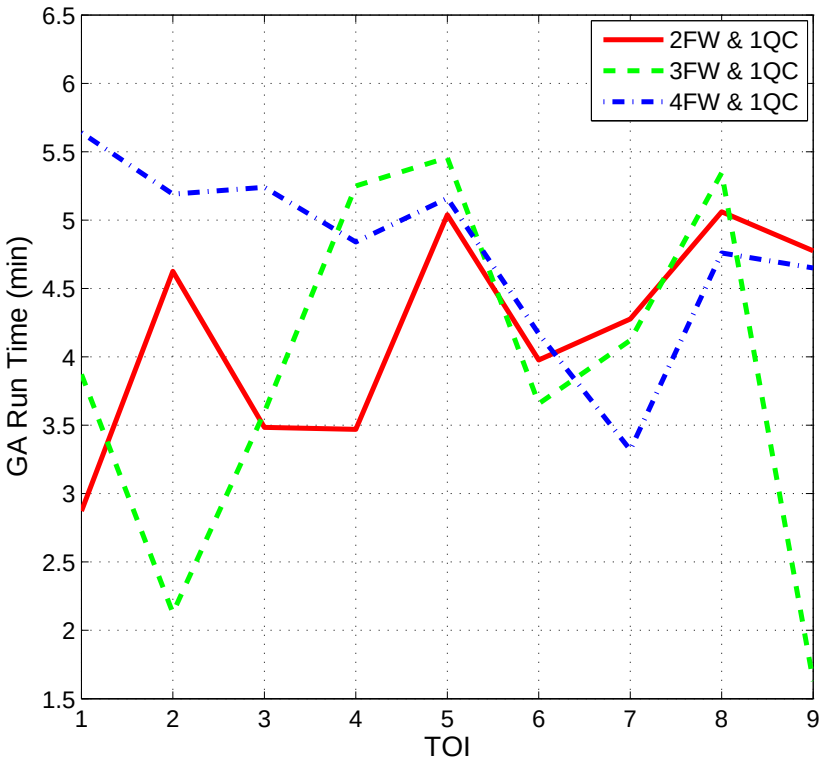

FIGURE 4.25: GA Mission Re-plan Run Times

Tables containing vehicle flight times and GA performance for all case studies can be found in the appendix in Tables A.1 through A.9.

Chapter 5

Conclusions

An adaptive mission planning system was developed to task a heterogeneous set of UAVs to investigate a TOI when it was located amongst a set of POIs being searched by a set of fixed wing aircraft. The developed system consisted of two GAs with fitness functions and flight path models that worked together to generate advanced mission plans. Two dimensional flight path models for a fixed wing aircraft and quadcopter were generated using a Dubins method. An initial fixed wing aircraft fitness functions was used to evaluate the efficiency of a mission plan for a homogeneous set of fixed wing aircraft. Missions in which POI visitation loads were balanced amongst the fixed wing aircraft were rewarded. Building off the initial fixed wing fitness function, a re-plan fixed wing fitness function was then developed to task fixed wing aircraft to visit POIs closest to their current position once a TOI was located. A quadcopter fitness function was then designed to task a quadcopter to visit the newly located. Quadcopter fitness function

was designed to maximize battery usage as it was desired that the quadcopter visit as many additional POIs as possible. Addition of the developed quadcopter fitness function to the GA ensured that additional surveillance of the TOI was obtained.

Case study simulations of missions were then conducted using varying numbers of fixed wing aircraft with a single quadcopter to ensure that the developed system generated plans that satisfied both initial and re-plan objectives. Simulation search space size was selected based on the flight distance range capabilities of a small fixed wing aircraft. Initial mission plans were obtained using the GA and the initial fixed wing fitness function and flight path planner. Mission re-plans were generated using the GA and a combination of the re-plan fixed wing fitness function, quadcopter fitness function and flight path planners.

Case study results indicated average overall mission time reductions of 30% with two fixed wing aircraft, 11% with three fixed wing aircraft and 7% with four fixed wing aircraft. Selected case study scenarios revealed that reductions in overall mission times were inversely proportional to the number of fixed wing aircraft used in the heterogeneous sets. In conclusion, the developed system will enable battlefield ground operators to plan a multi-UAV mission that provides additional surveillance of a TOI while reducing overall mission times.

5.1 Future Work

In addition to the research already conducted in this thesis, the following cases should be considered to benefit the adaptive mission planner:

1. Expanded case studies to further investigate the reduction in mission times with higher POIs, multiple TOIs and varying number of fixed wing and quadcopter platforms

2. The implementation of loitering path planners to obtain additional aerial surveillance around POI and TOIs.

3. Dynamic flight path planning algorithms to account for moving POIs, TOIs and obstacles.

4. Implementation of three dimensional path planning algorithms to better reflect fixed wing and quadcopter flight path behaviors.

Appendix A

Appendix

A.1 2 Fixed Wing + 1 Quadcopter Case Study Results

TOI	Initial Fixed Wing Time (min.)	Simulation Time Traveled (min.)	Re-Plan Fixed Wing Time (min.)	Fixed Wing Time Reduction	Mission Time Reduction w/ Quadcopter
1	31.94	10.89	7.84	41.35 %	29.91 %
2	33.13	4.99	15.07	39.48 %	27.99 %
3	31.76	8.48	9.58	43.12 %	29.64 %
4	32.77	9.05	8.86	45.38 %	31.30 %
5	32.52	2.40	14.09	49.28 %	36.32 %
6	32.61	7.59	10.57	44.30 %	31.01 %
7	32.81	6.10	14.57	36.99 %	26.26 %
8	32.24	3.00	15.84	41.60 %	29.65 %
9	32.19	4.32	15.89	37.21 %	25.50 %

Table A.1: Mission Time Reductions 2 Fixed Wing & 1 Quadcopter

		FW #1 (min.)	FW #2 (min.)	QC (min.)	AVG (min.)	Std Dev (min.)
TOI 1	I	15.88	16.06	-	15.97	0.126
	R	3.70	4.41	3.66	3.83	0.271
TOI 2	I	16.79	16.34	-	16.57	0.322
	R	7.47	7.59	3.81	6.29	2.153
TOI 3	I	15.98	15.78	-	15.88	0.140
	R	5.76	3.82	4.28	4.62	1.011
TOI 4	I	16.32	16.45	-	16.39	0.087
	R	4.54	4.32	4.61	4.49	0.155
TOI 5	I	16.24	16.27	-	16.26	0.024
	R	6.67	7.43	4.21	6.10	1.680
TOI 6	I	16.30	16.31	-	16.30	0.007
	R	4.50	6.07	4.33	4.97	0.960
TOI 7	I	16.36	16.46	-	16.41	0.071
	R	7.29	7.28	3.52	6.03	2.174
TOI 8	I	16.31	15.94	-	16.12	0.264
	R	7.94	7.90	3.85	6.56	2.347
TOI 9	I	16.05	16.14	-	16.10	0.067
	R	7.92	7.98	3.77	6.55	2.410

Table A.2: Flight Times 2 Fixed Wing & 1 Quadcopter

		Fitness	GA Run Time (min.)	Sec/-Gen	Convergence Time (min.)	Convergence Generation	ΔG
TOI 1	I	35.24	10.47	1.79	2.06	69	283
	R	90.99	2.87	0.49	1.41	172	180
TOI 2	I	36.15	11.23	1.92	5.90	184	168
	R	104.09	4.63	0.79	1.30	98	254
TOI 3	I	36.19	10.80	1.85	7.34	238	114
	R	88.72	3.48	0.60	3.13	314	38
TOI 4	I	36.00	10.42	1.79	7.00	235	117
	R	141.34	3.47	0.59	2.93	296	56
TOI 5	I	36.39	10.51	1.80	9.61	320	32
	R	101.64	5.04	0.86	2.74	190	162
TOI 6	I	34.65	11.53	1.98	6.16	187	165
	R	104.77	3.98	0.68	2.01	177	175
TOI 7	I	36.07	10.83	1.86	9.25	299	53
	R	98.44	4.28	0.73	2.35	192	160
TOI 8	I	35.40	11.08	1.90	8.52	269	83
	R	108.23	5.06	0.87	4.87	337	15
TOI 9	I	36.72	11.83	2.03	8.89	263	89
	R	97.55	4.77	0.82	1.31	96	256

Table A.3: GA Performance 2 Fixed Wing & 1 Quadcopter

A.2 3 Fixed Wing + 1 Quadcopter Case Study Results

TOI	Initial Fixed Wing Time (min.)	Simulation Time Traveled (min.)	Re-Plan Fixed Wing Time (min.)	Fixed Wing Time Reduction	Mission Time Reduction w/ Quadcopter
1	33.58	8.83	14.64	30.12 %	20.45 %
2	33.35	19.21	11.57	7.70 %	1.49 %
3	34.14	11.42	15.17	22.13 %	12.04 %
4	30.88	3.40	16.84	34.48 %	23.93 %
5	32.63	3.62	21.21	23.89 %	12.75 %
6	34.14	9.52	15.74	26.01 %	16.09 %
7	34.25	10.20	18.83	15.24 %	7.34 %
8	34.04	4.88	25.28	11.37 %	2.87 %
9	35.00	23.53	8.88	7.40 %	0.63 %

Table A.4: Mission Time Reductions 3 Fixed Wing & 1 Quadcopter

		FW #1 (min.)	FW #2 (min.)	FW #3 (min.)	QC (min.)	AVG (min.)	Std Dev (min.)
TOI 1	I	11.33	11.24	11.01	-	11.19	0.163
	R	5.09	4.89	4.66	3.25	4.47	0.835
TOI 2	I	11.09	11.09	11.16	-	11.12	0.038
	R	4.22	3.61	3.74	2.07	3.41	0.931
TOI 3	I	11.35	11.46	11.34	-	11.38	0.071
	R	4.42	4.95	5.80	3.45	4.65	0.985
TOI 4	I	10.34	10.28	10.26	-	10.29	0.045
	R	5.60	5.89	5.35	3.26	5.02	1.199
TOI 5	I	10.93	10.72	10.98	-	10.88	0.136
	R	6.94	6.80	7.48	3.63	6.21	1.744
TOI 6	I	10.90	11.59	11.64	-	11.38	0.411
	R	5.29	5.41	5.03	3.39	4.78	0.943
TOI 7	I	11.46	11.42	11.36	-	11.42	0.050
	R	5.83	6.00	7.00	2.70	5.38	1.859
TOI 8	I	11.28	10.99	11.77	-	11.35	0.396
	R	8.49	8.35	8.45	2.89	7.04	2.768
TOI 9	I	11.24	12.10	11.66	-	11.67	0.427
	R	2.01	3.70	3.17	2.37	2.81	0.763

Table A.5: Flight Times 3 Fixed Wing & 1 Quadcopter

		Fitness	GA Run Time (min.)	Sec/-Gen	Convergence Time (min.)	Convergence Generation	ΔG
TOI 1	I	37.62	8.80	1.51	8.60	342	10
	R	87.82	3.87	0.66	1.94	175	177
TOI 2	I	37.93	9.17	1.57	4.67	178	174
	R	72.16	2.13	0.36	0.66	109	243
TOI 3	I	38.87	9.28	1.59	3.45	130	222
	R	86.65	3.60	0.62	3.57	347	5
TOI 4	I	36.86	8.81	1.51	7.05	280	72
	R	90.23	5.25	0.90	5.04	336	16
TOI 5	I	37.31	9.51	1.63	4.54	167	185
	R	92.77	5.46	0.94	4.40	282	70
TOI 6	I	39.35	9.32	1.60	6.45	242	110
	R	88.26	3.66	0.63	2.78	266	186
TOI 7	I	38.44	9.07	1.56	5.08	196	156
	R	85.60	4.12	0.71	2.25	191	161
TOI 8	I	37.34	9.58	1.64	1.59	58	294
	R	93.38	5.35	0.92	3.07	201	151
TOI 9	I	39.00	9.23	1.58	8.07	306	46
	R	35.25	1.63	0.28	0.25	53	299

Table A.6: GA Performance 3 Fixed Wing & 1 Quadcopter

A.3 4 Fixed Wing + 1 Quadcopter Case Study Results

TOI	Initial Fixed Wing Time (min.)	Simulation Time Traveled (min.)	Re-Plan Fixed Wing Time (min.)	Fixed Wing Time Reduction	Mission Time Reduction w/ Quadcopter
1	33.80	3.32	26.41	16.98 %	9.11 %
2	36.03	7.02	25.29	10.35 %	2.41 %
3	35.41	5.69	25.84	10.97 %	2.05 %
4	33.24	4.54	19.66	27.20 %	17.01 %
5	34.07	4.83	24.04	15.26 %	6.29 %
6	34.33	8.27	19.92	17.88 %	9.23 %
7	36.04	14.04	15.35	18.47 %	10.17 %
8	33.61	6.88	24.68	6.08 %	-1.91 %
9	36.35	7.22	23.66	15.03 %	7.21 %

Table A.7: Mission Time Reductions 4 Fixed Wing & 1 Quadcopter

		FW #1 (min.)	FW #2 (min.)	FW #3 (min.)	FW #4 (min.)	QC (min.)	AVG (min.)	Std Dev (min.)
TOI 1	I	8.35	8.80	9.40	9.25	-	8.95	0.475
	R	7.36	5.86	6.80	6.39	2.82	5.84	1.781
TOI 2	I	8.51	8.51	9.46	9.56	-	9.01	0.578
	R	6.74	7.01	6.24	5.30	2.86	5.63	1.679
TOI 3	I	9.17	9.14	8.70	8.40	-	8.85	0.372
	R	5.94	6.95	6.95	5.99	3.16	5.80	1.556
TOI 4	I	8.65	6.65	7.92	8.01	-	8.31	0.396
	R	5.64	4.80	5.66	3.55	3.39	4.61	1.099
TOI 5	I	9.15	8.98	8.75	7.19	-	8.52	0.899
	R	5.37	6.87	6.41	5.39	3.05	5.42	1.473
TOI 6	I	8.26	8.96	8.24	8.87	-	8.58	0.384
	R	5.29	4.97	5.13	4.53	2.97	4.58	0.944
TOI 7	I	8.61	9.38	9.24	8.81	-	9.01	0.361
	R	3.92	3.72	4.78	2.93	2.99	3.67	0.760
TOI 8	I	8.25	8.53	8.30	8.53	-	8.40	0.148
	R	6.78	7.32	6.69	3.90	2.69	5.47	2.051
TOI 9	I	9.25	9.18	8.64	9.28	-	9.09	0.300
	R	6.77	6.26	6.54	4.10	2.84	5.30	1.740

TABLE A.8: Flight Times 4 Fixed Wing & 1 Quadcopter

		Fitness	GA Run Time (min.)	Sec/-Gen	Convergence Time (min.)	Convergence Generation	ΔG
TOI 1	I	40.42	8.00	1.37	7.61	333	19
	R	85.97	5.64	0.97	4.95	307	45
TOI 2	I	40.57	8.47	1.45	2.95	122	230
	R	98.15	5.19	0.89	3.20	216	136
TOI 3	I	41.23	8.47	1.45	7.94	328	24
	R	92.83	5.24	0.90	2.54	170	182
TOI 4	I	39.52	8.04	1.38	4.11	179	173
	R	96.42	4.84	0.83	3.34	242	110
TOI 5	I	37.99	8.37	1.43	4.90	205	147
	R	92.46	5.16	0.89	4.50	305	47
TOI 6	I	39.92	8.26	1.42	6.33	268	84
	R	95.03	4.17	0.72	1.66	139	213
TOI 7	I	41.56	8.33	1.43	4.07	171	181
	R	82.95	3.32	0.57	1.00	105	247
TOI 8	I	40.30	7.78	1.33	7.49	337	15
	R	99.06	4.76	0.82	3.91	288	64
TOI 9	I	40.68	8.42	1.44	3.23	134	218
	R	99.34	4.65	0.80	3.55	267	85

Table A.9: GA Performance 4 Fixed Wing & 1 Quadcopter

Bibliography

[1] 3DRobotics Inc. Aero, 2015. URL https://store.3drobotics.com/products/3DR-Aero.

[2] 3D Robotics Inc. Iris+, 2015. URL https://store.3drobotics.com/products/iris.

[3] Yanushevsky R. *Guidance of Unmanned Aerial Vehicles*. CRC Press Taylor & Francis Group, 2011.

[4] Valavanis K. P. *Advances in Unmanned Aerial Vehicles: State of the Art and the Road to Autonomy*. Springer Publishing Company, Incorporated, 1st edition, 2007.

[5] Lozano R. *Unmanned Aerial Vehicles: Embedded Control*, chapter 1. Wiley, 2010.

[6] Fact sheet: Rq-11b raven system. Technical report, Air Force Special Operations Command Public Affairs Office, 2009. URL http://www.avinc.com/downloads/USAF_Raven_FactSheet.pdf.

[7] Gopichand A., Anasuya B.D.P.P.S.L., Yamini C., Vaidehi N.N., and Venkata Y.R. Modelling and analysis of multicopter frame and propeller. *International Journal of Research in Engineering and Technology*, 02(04), 2013.

[8] Aeryon scout, 2015. URL http://www.aeryon.com/products/avs/aeryon-scout.html.

[9] Wolsey L. A. and Nemhauser G. L. Integer and combinatorial optimization. In *Wiley Series in Discrete Mathematics and Optimization*, volume 55, pages 27–49. Wiley, 2004.

[10] Richards A., Bellingham J., Tillerson M., and How J. Coordination and control of multiple uavs. In *AIAA Guidance, Navigation, and Control Conference and Exhibit*, 2002.

[11] Schumacher C., Chandler P., Pachter M., and Pachter L. Constrained optimization for uav task assignment. In *AIAA Guidance, Navigation, and Control Conference and Exhibit*, 2004.

[12] Darrah M. A., Niland W. M., and Stolarik B. M. Multiple uav dynamic task allocation using mixed integer linear programming in sead mission. In *Proc. AIAA Infotech@Aerospace Conference*, 2005.

[13] Wang J., Zhang Y.F., Geng L., Fuh J.Y.H, and Teo S.H. A heuristic mission planning algorithm for heterogeneous tasks with heterogeneous uavs. *Unmanned Systems Journal*, 3:205–219, 2015.

[14] Leary S., Deittert M., and Bookless J. Constrained uav mission planning: A comparison of approaches. In *2011 IEEE International Conference on Computer Vision Workshop*, 2011.

[15] Misa T.J. and Frana P.L. An interview with Edsger W. Dijkstra. *Commun. ACM*, 53(8):41–47, August 2010.

[16] Felner A. Position paper: Dijkstra's algorithm versus uniform cost search or a case against Dijkstra's algorithm. In *Proceedings of The Fourth International Symposium on Combinatorial*, 2011.

[17] Razavi R. How routing algorithms work, 2015. URL http://computer.howstuffworks.com/routing-algorithm2.htm.

[18] Jehn-Ruey J., Hsin-Wen H., Ji-Hau L., and Szu-Yuan C. Extending Dijkstra's shortest path algorithm for software defined networking. In *2014 16th Asia-Pacific Network Operations and Management Symposium (APNOMS)*, pages 1–4, Sept 2014.

[19] Sudhakar T.D., Vadivoo N.S., Slochanal S.M.R., and Ravichandran S. Supply restoration in distribution networks using Dijkstra's algorithm. In *2004 International Conference on Power System Technology (PowerCon 2004)*, volume 1, pages 640–645, Nov 2004.

[20] Eklund P.W., Kirkby S., and Pollitt S. A dynamic multi-source Dijkstra's algorithm for vehicle routing. In *Australian and New Zealand Conference on Intelligent Information Systems*, pages 329–333, Nov 1996.

[21] Sivanandam S.N. and Deepa S.N. *Introduction to Genetic Algorithms*. Springer, 2008.

[22] Man K.F., Tang K.S., and Kwong S. Genetic algorithms: Concepts and applications. *IEEE Transactions on Industrial Electronics*, 43(5):519–534, Oct 1996.

[23] Goldberg D.E. *Genetic Algorithms in Search, Optimization and Machine Learning*. Addison-Wesley Longman Publishing Co., Inc., 1st edition, 1989.

[24] Tian J., Shen L., and Zheng Y. Genetic algorithm based approach for multi-uav cooperative reconnaissance mission planning problem. In *Foundations of Intelligent Systems*, volume 4203, pages 101–110. Springer Berlin Heidelberg, 2006.

[25] Darrah M., Fuller E., Munasinghe T., Duling K., Gautam M., and Wathen M. Using genetic algorithms for tasking teams of raven uavs. *Journal of Intelligent & Robotic Systems*, 70(1-4):361–371, 2013.

[26] Darrah M., Wilhelm J., Munasinghe T., Duling K., Yokum S., Sorton E., Rojas J., and M. Wathen. A flexible genetic algorithm system for multi-uav surveillance: Algorithm and flight testing. *Unmanned Systems*, 03(01):49–62, 2015.

[27] LaValle S.M. *Planning Algorithms*. Cambridge University Press, 2006.

[28] Riviere S. and Schmitt D. Two-dimensional line space Voronoi diagram. In *Voronoi Diagrams in Science and Engineering, 2007. ISVD '07. 4th International Symposium*, pages 168–175, July 2007.

[29] Bhattacharya P. and Gavrilova M.L. Roadmap-based path planning - using the Voronoi diagram for a clearance-based shortest path. *Robotics Automation Magazine, IEEE*, 15(2):58–66, June 2008.

[30] Xia C. and Xiangmin C. The uav dynamic path planning algorithm research based on Voronoi diagram. In *The 26th Chinese Control and Decision Conference*, pages 1069–1071, May 2014.

[31] Davis J., Perhinschi M., Wilburn B., and Karas O. Development of a modified Voronoi algorithm for uav path planning and obstacle avoidance. In *AIAA Guidance, Navigation, and Control Conference*, 2012.

[32] Araujo J.F., Sujit P.B., and Sousa J.B. Multiple uav area decomposition and coverage. In *2013 IEEE Symposium on Computational Intelligence for Security and Defense Applications (CISDA)*, pages 30–37, April 2013.

[33] Perhinschi M., Moncayo H., Davis J., Wilburn B., Karas O., and Wathen M. Development of a simulation environment for autonomous flight control algorithms. In *AIAA Modeling and Simulation Technologies Conferenec*, 2011.

[34] L E. Dubins. On curves of minimal length with a constraint on average curvature, and with prescribed initial and terminal positions and tangents. *American Journal of Mathematics*, 79:497–516, 1957.

[35] Grymin D.J. and Crassidis A.L. Simplified model development and trajectory determination for a uav using the Dubins set. In *AIAA Atmospheric Flight Mechanics Conference*, 2009.

[36] Karas O. Uav simulation environment for autonomous flight control algorithms. Master's thesis, West Virginia University, 2012.

[37] Wilburn J. *Development of an Integrated Intelligent Multi -Objective Framework for UAV Trajectory Generation.* PhD thesis, West Virginia University, 2013.

[38] Shanmugavel M., Tsourdos A., White B., and Żbikowski R. Co-operative path planning of multiple uavs using Dubins paths with clothoid arcs. *Control Engineering Practice*, 18(09):41084 – 1092, 2010.

[39] Al Nuaimi M. Analysis and comparison of Clothoid and Dubins algorithms for uav trajectory generation. Master's thesis, West Virginia University, 2014.